

## Supplementary Information

### **One-Dimensional Palladium Wires: Influence of Molecular Changes on Supramolecular Structure**

Michael G. Campbell, Shao-Liang Zheng, and Tobias Ritter\*

Department of Chemistry and Chemical Biology, Harvard University

Cambridge, Massachusetts 02138

E-mail: [ritter@chemistry.harvard.edu](mailto:ritter@chemistry.harvard.edu)

## Table of Contents

Materials and Methods .....	3
Experimental Data .....	4
Experimental Procedures and Compound Characterization .....	4
Benzo[ <i>h</i> ]quinolinyll Palladium Acetate Dimer ( <b>1</b> ).....	4
Palladium(III) Wire <b>2</b> .....	4
Palladium(2.5) Wire <b>3</b> .....	5
Pd(III) Wire <b>4</b> .....	6
7-Nitrobenzo[ <i>h</i> ]quinoline ( <b>S1</b> ) .....	6
7-Aminobenzo[ <i>h</i> ]quinoline ( <b>S2</b> ).....	7
7-Chlorobenzo[ <i>h</i> ]quinoline ( <b>S3</b> ).....	8
7-Chlorobenzo[ <i>h</i> ]quinolinyll Palladium Acetate Dimer ( <b>5</b> ).....	8
Pd(2.5) Wire <b>6</b> .....	9
[(7-Cl-bhq)Pd(OAc)F] <sub>2</sub> ( <b>7</b> ).....	10
X-ray Crystallography Data.....	11
General Procedure for X-ray Data Collection and Refinement.....	11
Pd(III) Wire <b>4</b> (CCDC 952240).....	12
Pd(2.5) Wire <b>6</b> (CCDC 952241).....	16
Pd(III) Fluoride Dimer <b>7</b> (CCDC 952242) .....	21
DFT Calculations .....	26
Cartesian Coordinates for the Optimized Structure of <b>7</b> .....	27
Simulated UV-vis Spectrum for <b>7</b> .....	28
NMR Data.....	31
UV-vis/NIR Data .....	43
UV-vis Spectrum of <b>1</b> (CH <sub>2</sub> Cl <sub>2</sub> , 23 °C) .....	43
UV-vis/NIR Spectrum of <b>2</b> (CH <sub>2</sub> Cl <sub>2</sub> , 0 °C) .....	44
UV-vis/NIR Spectrum of <b>3</b> (CH <sub>2</sub> Cl <sub>2</sub> , 0 °C) .....	46
UV-vis/NIR Spectrum of <b>6</b> (CH <sub>2</sub> Cl <sub>2</sub> , 5 °C) .....	48
UV-vis/NIR Spectrum of <b>7</b> (CH <sub>2</sub> Cl <sub>2</sub> , 5 °C) .....	50

## Materials and Methods

All manipulations were carried out in a dry box under a N<sub>2</sub> atmosphere unless otherwise noted. Anhydrous solvents (pentane, ether, CH<sub>2</sub>Cl<sub>2</sub>) were obtained by filtration through drying columns<sup>1</sup> on an mBraun system, and were degassed by three freeze-pump-thaw cycles before use. Purified compounds were dried under high vacuum (0.01–0.05 Torr); yields refer to purified and spectroscopically pure compounds. NMR spectra were recorded on either a Varian Unity/Inova 500 spectrometer operating at 500 MHz and 125 MHz for <sup>1</sup>H and <sup>13</sup>C acquisitions, respectively, or a Varian Mercury 400 spectrometer operating at 400 MHz and 375 MHz for <sup>1</sup>H and <sup>19</sup>F acquisitions, respectively. Chemical shifts are reported in ppm with the solvent resonance as the internal standard. The following solvent chemical shifts were used as reference values<sup>2</sup> (ppm): CDCl<sub>3</sub> = 7.26 (<sup>1</sup>H), 77.16 (<sup>13</sup>C); CD<sub>2</sub>Cl<sub>2</sub> = 5.32 (<sup>1</sup>H), 53.84 (<sup>13</sup>C). Data are reported as follows: s = singlet, br = broad, d = doublet, t = triplet, q = quartet, quin = quintet, m = multiplet; coupling constants in Hz; integration. High-resolution mass spectra were obtained on Jeol AX-505 or SX-102 spectrometers at the Harvard University Mass Spectrometry Facilities. UV-vis/NIR spectra were measured on a Perkin Elmer Lambda 750 spectrophotometer or a Varian Cary 5000 spectrophotometer. Pd(OAc)<sub>2</sub> was purchased from Strem. XeF<sub>2</sub> was purchased from Matrix Scientific. Benzo[*h*]quinoline was purchased from TCI America. All reagents were dried overnight in a vacuum desiccator or with heating under dynamic vacuum before being transferred into a dry box (except for XeF<sub>2</sub>, which was received packed under argon and was transferred into a dry box without further treatment).

### Acknowledgement:

This research was supported in part by an award from the Department of Energy (DOE) Office of Science Graduate Fellowship Program (DOE SCGF). The DOE SCGF Program was made possible in part by the American Recovery and Reinvestment Act of 2009. The DOE SCGF program is administered by the Oak Ridge Institute for Science and Education for the DOE. ORISE is managed by Oak Ridge Associated Universities (ORAU) under DOE contract number DE-AC05-06OR23100. All opinions expressed in this paper are the authors' and do not necessarily reflect the policies and views of DOE, ORAU, or ORISE.

---

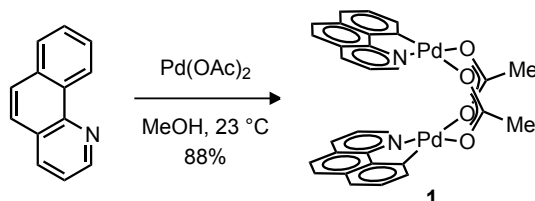
<sup>1</sup> Pangborn, A. B.; Giardello, M. A.; Grubbs, R. H.; Rosen, R. K.; Timmers, F. J. *Organometallics* **1996**, *15*, 518.

<sup>2</sup> Fulmer, G. R.; Miller, A. J. M.; Sherden, N. H.; Gottlieb, H. E.; Nudelman, A.; Stoltz, B. M.; Bercaw, J. E.; Goldberg, K. I. *Organometallics* **2010**, *29*, 2176-2179.

## Experimental Data

### Experimental Procedures and Compound Characterization

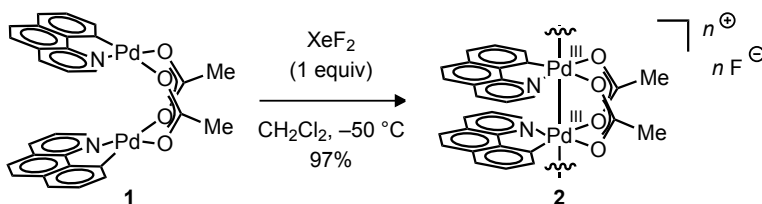
#### Benzo[*h*]quinolinyll Palladium Acetate Dimer (**1**)<sup>3</sup>



To benzo[*h*]quinoline (1.00 g, 5.58 mmol, 1.00 equiv) in MeOH (75 mL) at 23 °C under air was added  $\text{Pd}(\text{OAc})_2$  (1.25 g, 5.58 mmol, 1.00 equiv). After stirring for eight hours, the precipitate was isolated by filtration and washed sequentially with MeOH (50 mL) and Et<sub>2</sub>O (50 mL) to afford 1.68 g of the title compound as a yellow solid (88% yield).

NMR spectroscopy: <sup>1</sup>H-NMR (500 MHz, CDCl<sub>3</sub>, 23 °C,  $\delta$ ): 7.82 (dd,  $J$  = 5.0 Hz, 1.1 Hz, 2H), 7.44 (dd,  $J$  = 8.0 Hz, 1.1 Hz, 2H), 7.25–7.20 (m, 6H), 7.09 (dd,  $J$  = 6.9 Hz, 1.1 Hz, 2H), 6.99 (d,  $J$  = 8.7 Hz, 2H), 6.48 (dd,  $J$  = 8.0 Hz, 5.0 Hz, 2H), 2.38 (s, 6H). <sup>13</sup>C-NMR (125 MHz, CDCl<sub>3</sub>, 23 °C,  $\delta$ ): 182.3, 152.9, 148.6, 148.5, 139.7, 135.0, 132.2, 128.7, 127.6, 127.4, 124.7, 122.6, 121.8, 119.5, 24.9. These spectroscopic data correspond to the reported data in reference 3. UV-VIS Spectroscopy (CH<sub>2</sub>Cl<sub>2</sub>, 23 °C): 377 nm ( $\epsilon$  =  $2.39 \times 10^3 \text{ M}^{-1} \text{ cm}^{-1}$ ); 346 nm ( $\epsilon$  =  $2.30 \times 10^3 \text{ M}^{-1} \text{ cm}^{-1}$ ).

#### Palladium(III) Wire **2**<sup>4</sup>



Benzo[*h*]quinolinyll palladium acetate dimer (**1**) (21 mg,  $3.1 \times 10^{-5}$  mol, 1.0 equiv) was dissolved in 1.0 mL CH<sub>2</sub>Cl<sub>2</sub> at -50 °C.  $\text{XeF}_2$  (5.3 mg,  $3.1 \times 10^{-5}$  mol, 1.0 equiv) was added as a solid in one portion. The yellow solution immediately became a dark red-brown suspension. After stirring for five minutes at -50 °C, solvent was removed *in vacuo* at -50 °C. The residue was washed

<sup>3</sup> Dick, A. R., Hull, K. L. & Sanford, M. S. *J. Am. Chem. Soc.* **2004**, 126, 2300–2301.

<sup>4</sup> Campbell, M. G.; Powers, D. C.; Raynaud, J.; Graham, M. J.; Xie, P.; Lee, E.; Ritter, T. *Nat. Chem.* **2011**, 3, 949–953.

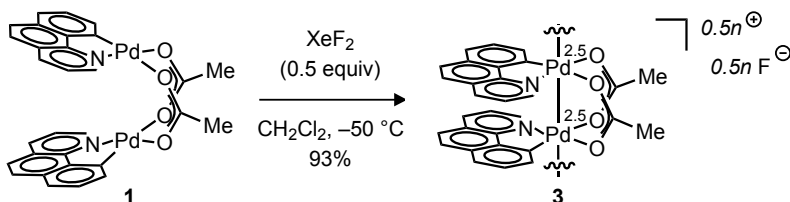
with Et<sub>2</sub>O (1.0 mL) at –50 °C. The Et<sub>2</sub>O was decanted, and the residue was dried *in vacuo* (approx. 50 mTorr) at –50 °C to afford 22 mg of the title compound (97% yield) as a dark red solid.

NMR Spectroscopy: <sup>1</sup>H-NMR (500 MHz, CD<sub>2</sub>Cl<sub>2</sub>, –10 °C, δ): 7.87 (d, *J* = 5.1 Hz, 2H), 7.71 (d, *J* = 7.7 Hz, 2H), 7.47–7.40 (m, 4H), 7.35 (d, *J* = 8.4 Hz, 2H), 7.27 (d, *J* = 7.0 Hz, 2H), 7.15 (d, *J* = 8.8 Hz, 2H), 6.86 (dd, *J* = 4.8 Hz, *J* = 4.8 Hz, 2H), 2.72 (s, 6H). <sup>19</sup>F-NMR (375 MHz, CD<sub>2</sub>Cl<sub>2</sub>, –10 °C, δ): –170.4 (br s). UV-VIS Spectroscopy (CH<sub>2</sub>Cl<sub>2</sub>, 0 °C): 1021 nm (absorbance at this wavelength is non-linear with concentration; see ‘UV-vis Data’ section for details); 464 nm (absorbance at this wavelength is non-linear with concentration); 376 nm ( $\epsilon = 2.47 \times 10^3 \text{ M}^{-1} \text{ cm}^{-1}$ ). Thermal instability prevented both meaningful mass spectrometry as well as elemental analysis from being obtained. <sup>13</sup>C NMR signals were not observed.

These spectroscopic data correspond to the data reported in reference 4.

X-ray quality crystals of **2** were obtained as follows: at –50 °C, a solution of approximately 20 mg of **2** in 1.0 mL CH<sub>2</sub>Cl<sub>2</sub> was filtered through glass wool into two 2.0 mL plastic vials at –50 °C. Pre-cooled pentane (–50 °C) was carefully layered on top of the solution containing **2**. The vials were stored at –35 °C for 24 hours, at which point red needle crystals of **2** were observed. Redissolved crystals of **2** in CD<sub>2</sub>Cl<sub>2</sub> displayed <sup>1</sup>H and <sup>19</sup>F NMR spectra that were identical to freshly prepared samples of **2**.

#### Palladium(2.5) Wire **3**<sup>4</sup>



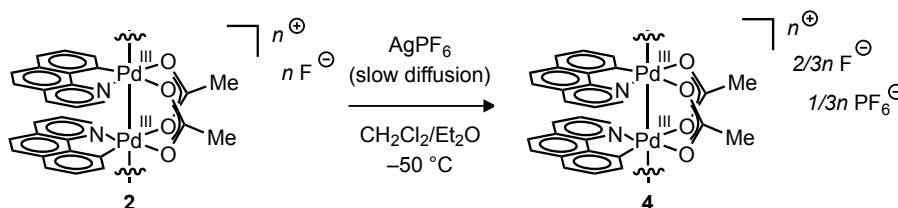
Benzo[*h*]quinolinylnyl palladium acetate dimer (**1**) (20. mg,  $2.9 \times 10^{-5}$  mol, 1.0 equiv) was dissolved in 1.0 mL CH<sub>2</sub>Cl<sub>2</sub> at –50 °C. XeF<sub>2</sub> (2.5 mg,  $1.5 \times 10^{-5}$  mol, 0.50 equiv) was added as a solid in one portion. The yellow solution immediately became dark red-brown. After stirring for five minutes at –50 °C, solvent was removed *in vacuo*. The residue was triturated with pentane (2 × 1 mL) at –50 °C. The pentane was decanted, and the residue was dried *in vacuo* (approx. 50 mTorr) at –50 °C to afford 19 mg of the title compound (93% yield) as a dark red-brown solid.

NMR Spectroscopy: <sup>1</sup>H NMR (400 MHz, CD<sub>2</sub>Cl<sub>2</sub>, –25 °C, δ): 7.85 (d, *J* = 5.9 Hz, 2H), 7.73 (d, *J* = 8.8 Hz, 2H), 7.47–7.17 (m, 10H), 6.85 (br, 2H), 2.71 (s, 6H). <sup>19</sup>F NMR (375 MHz, CD<sub>2</sub>Cl<sub>2</sub>, –25 °C, δ): –213.2 (br s, *h*<sub>1/2</sub> = 440 Hz). UV-Vis Spectroscopy (CH<sub>2</sub>Cl<sub>2</sub>, 0 °C): 991 nm (absorbance at this wavelength is non-linear with concentration); 374 nm ( $\epsilon = 2.29 \times 10^3 \text{ M}^{-1} \text{ cm}^{-1}$ ); 345 nm ( $\epsilon = 2.27 \times 10^3 \text{ M}^{-1} \text{ cm}^{-1}$ ). Thermal instability prevented both meaningful mass spectrometry as well as elemental analysis from being obtained. <sup>13</sup>C NMR signals were not observed.

These spectroscopic data correspond to the data reported in reference 4.

X-ray quality crystals of **3** were obtained as follows: at  $-50\text{ }^{\circ}\text{C}$ , 0.5 mL of a 10 mg/mL solution of **3** in  $\text{CH}_2\text{Cl}_2$  was filtered through glass wool into a 2.0 mL plastic vial. Pentane (1.5 mL, pre-cooled to  $-50\text{ }^{\circ}\text{C}$ ) was carefully layered on top of the solution containing **3**. The vial was stored at  $-35\text{ }^{\circ}\text{C}$  for 24 hours, at which point long, red needle crystals of **3** were observed. Redissolved crystals of **3** in  $\text{CD}_2\text{Cl}_2$  displayed  $^1\text{H}$  and  $^{19}\text{F}$  NMR spectra identical to freshly prepared **3**.

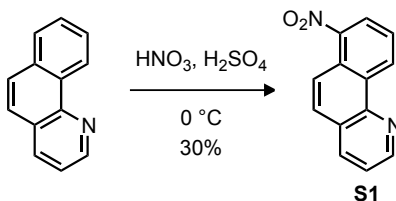
#### Pd(III) Wire **4**



A 10 mg/mL solution of Pd(III) Wire **2** (0.5 mL) at  $-50\text{ }^{\circ}\text{C}$  was divided into three glass tubes ( $6 \times 50\text{ mm}$ ), pre-cooled to  $-50\text{ }^{\circ}\text{C}$ . The solution of **2** was layered with a small amount of benzene ( $\sim 50\text{ }\mu\text{L}$ ), which was allowed to freeze into a solid wafer. On top of the frozen benzene was layered an 8 mg/mL solution of  $\text{AgPF}_6$  in  $\text{Et}_2\text{O}$ , pre-cooled to  $-50\text{ }^{\circ}\text{C}$  (optimal results were obtained when the ratio of solutions of **2**: $\text{AgPF}_6$  was approximately 1:5). The tubes were capped and stored at  $-35\text{ }^{\circ}\text{C}$  for three days, at which point dark blue needle crystals were observed. X-ray crystallographic analysis of these crystals revealed Pd(III) wire **4**; full details are included in the X-ray Crystallography Data section.

Crystals of the title compound were insoluble in non-coordinating solvents such as  $\text{CD}_2\text{Cl}_2$ , therefore we were unable to obtain meaningful solution-state spectroscopic data of the 1-D wires. Attempts to redissolve crystals of **4** in coordinating solvents such as  $\text{CD}_3\text{CN}$  led to decomposition.

#### 7-Nitrobenzo[*h*]quinoline (**S1**)<sup>56</sup>



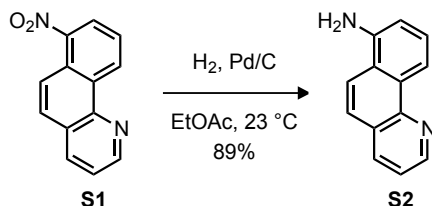
<sup>5</sup> Barltrop, J. A.; MacPhee, K. E. *J. Chem. Soc.* **1952**, 638–642.

<sup>6</sup> Furuya, T.; Benitez, D.; Tkatchouk, E.; Strom, A. E.; Tang, P.; Goddard, W. A., III; Ritter, T. *J. Am. Chem. Soc.* **2010**, *132*, 3793–3807.

Benzo[*h*]quinoline (5.00 g, 27.9 mmol, 1.00 equiv) was dissolved in conc. H<sub>2</sub>SO<sub>4</sub> (10 mL) at 23 °C under air. The reaction mixture was cooled to 0 °C and a mixture of conc. H<sub>2</sub>SO<sub>4</sub> (3.3 mL) and HNO<sub>3</sub> (5.3 mL) (prepared with cooling) was added drop-wise over 20 min. The reaction mixture was stirred at 0 °C for 15 min and was subsequently poured onto water (300 mL) with vigorous stirring, causing the precipitation of yellow solids. The precipitate was filtered, dried, and purified by chromatography on silica gel eluting with a gradient from CH<sub>2</sub>Cl<sub>2</sub>/hexanes 1:1 (v/v) to 100% CH<sub>2</sub>Cl<sub>2</sub>, affording 1.88 g of the title compound as a pale yellow solid (30% yield).

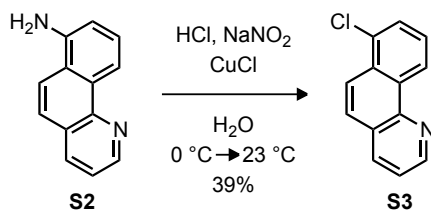
$R_f$  = 0.78 (CH<sub>2</sub>Cl<sub>2</sub>). NMR Spectroscopy: <sup>1</sup>H NMR (500 MHz, CDCl<sub>3</sub>, 25 °C,  $\delta$ ): 9.65 (d,  $J$  = 8.0 Hz, 1H), 9.03 (dd,  $J$  = 4.5 Hz,  $J$  = 2.0 Hz, 1H), 8.43 (d,  $J$  = 9.5 Hz, 1H), 8.32 (dd,  $J$  = 7.5 Hz,  $J$  = 1.0 Hz, 1H), 8.21 (dd,  $J$  = 8.0 Hz,  $J$  = 1.5 Hz, 1H), 7.88 (d,  $J$  = 9.0 Hz, 1H), 7.77 (dd,  $J$  = 8.0 Hz,  $J$  = 8.0 Hz, 1H), 7.61 (dd,  $J$  = 8.0 Hz,  $J$  = 4.5 Hz, 1H). <sup>13</sup>C NMR (125 MHz, CDCl<sub>3</sub>, 25 °C,  $\delta$ ): 149.9, 146.9, 145.3, 135.9, 132.9, 130.4, 129.0, 125.9, 125.6, 125.6, 125.1, 123.0, 121.3. Mass Spectrometry: HRMS-FIA ( $m/z$ ): Calcd for [C<sub>13</sub>H<sub>9</sub>N<sub>2</sub>O<sub>2</sub>]<sup>+</sup> ([M+H]<sup>+</sup>), 225.06585. Found, 225.06650. These spectroscopic data correspond to the reported data in reference 6.

#### 7-Aminobenzo[*h*]quinoline (S2)<sup>6</sup>



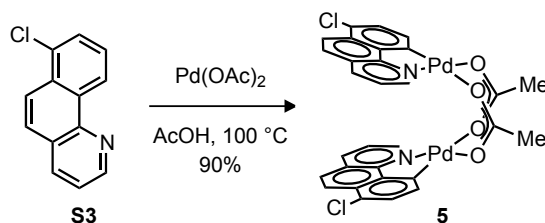
To 7-nitrobenzo[*h*]quinoline (**S1**) (810 mg, 3.61 mmol, 1.00 equiv) in EtOAc (36 mL) at 23 °C under air was added 10% Pd/C (361 mg). H<sub>2</sub> gas (1 atm) was introduced using a balloon and the reaction mixture was stirred for 1 hour at 23 °C. The reaction mixture was filtered through a pad of celite and the filtrate was concentrated to afford 628 mg of the title compound as a brown solid (89% yield).

$R_f$  = 0.30 (CH<sub>2</sub>Cl<sub>2</sub>). NMR Spectroscopy: <sup>1</sup>H NMR (500 MHz, CDCl<sub>3</sub>, 23 °C,  $\delta$ ): 8.99 (dd,  $J$  = 4.0 Hz,  $J$  = 1.5 Hz, 1H), 8.79 (d,  $J$  = 8.5 Hz, 1H), 8.13 (dd,  $J$  = 8.0 Hz, 1.5 Hz, 1H), 7.82 (d,  $J$  = 9.0 Hz, 1H), 7.62 (d,  $J$  = 9.5 Hz, 1H), 7.54 (dd,  $J$  = 7.5 Hz,  $J$  = 7.5 Hz, 1H), 7.49 (dd,  $J$  = 8.0 Hz,  $J$  = 4.5 Hz, 1H), 7.02 (dd,  $J$  = 7.5 Hz,  $J$  = 1.0 Hz, 1H), 4.19 (br s, 2H). <sup>13</sup>C NMR (125 MHz, CDCl<sub>3</sub>, 25 °C,  $\delta$ ): 146.8, 146.7, 142.4, 135.7, 132.5, 127.5, 126.1, 124.0, 122.4, 121.7, 120.5, 115.3, 113.5. Mass Spectrometry: HRMS-FIA ( $m/z$ ): Calcd for [C<sub>13</sub>H<sub>11</sub>N<sub>2</sub>]<sup>+</sup> ([M+H]<sup>+</sup>), 195.09222. Found, 195.09235. These spectroscopic data correspond to the reported data in reference 6.

**7-Chlorobenzo[*h*]quinoline (S3)<sup>6</sup>**

7-Aminobenzo[*h*]quinoline (**S2**) (188 mg, 0.968 mmol, 1.00 equiv) was dissolved in 2N HCl (5.6 mL) at 0 °C under air. To the reaction mixture was added a solution of NaNO<sub>2</sub> (80.1 mg, 1.16 mmol, 1.20 equiv) in H<sub>2</sub>O (1.5 mL) drop-wise. The reaction mixture was stirred for 30 min at 0 °C and a solution of CuCl (95.8 mg, 0.968 mmol, 1.00 equiv) in conc. HCl (2.4 mL) was added drop-wise over 2 min. The reaction mixture was allowed to slowly warm to 23 °C with further stirring for 3 hours before saturated aqueous NaHCO<sub>3</sub> (~15 mL) was added to adjust pH to ~7. To the reaction mixture was added CH<sub>2</sub>Cl<sub>2</sub> (20 mL) and the phases were separated. The aqueous layer was extracted with CH<sub>2</sub>Cl<sub>2</sub> (2 × 20 mL). The combined organic phases were washed with brine (20 mL) and dried (Na<sub>2</sub>SO<sub>4</sub>). The filtrate was concentrated *in vacuo* and the residue was purified by chromatography on silica gel eluting with CH<sub>2</sub>Cl<sub>2</sub>/hexanes 2:1 (v/v) to afford 81.0 mg of the title compound as a pale-yellow solid (39% yield).

*R*<sub>f</sub> = 0.79 (CH<sub>2</sub>Cl<sub>2</sub>). NMR Spectroscopy: <sup>1</sup>H NMR (500 MHz, CDCl<sub>3</sub>, 25 °C, δ): 9.26 (d, *J* = 8.5 Hz, 1H), 9.02 (dd, *J* = 4.5 Hz, *J* = 2.0 Hz, 1H), 8.27 (d, *J* = 9.5 Hz, 1H), 8.19 (dd, *J* = 8.0 Hz, *J* = 2.0 Hz, 1H), 7.79–7.76 (m, 2H), 7.64 (dd, *J* = 8.5 Hz, *J* = 8.5 Hz, 1H), 7.55 (dd, *J* = 8.0 Hz, *J* = 4.5 Hz, 1H). <sup>13</sup>C NMR (125 MHz, CDCl<sub>3</sub>, 25 °C, δ): 149.3, 146.1, 135.9, 133.1, 131.9, 130.8, 128.6, 127.0, 126.5, 126.2, 123.4, 123.4, 122.3. Mass Spectrometry: HRMS-FIA (*m/z*): Calcd for [C<sub>13</sub>H<sub>9</sub>ClN]<sup>+</sup> ([M+H]<sup>+</sup>), 214.04235. Found, 214.04200. These spectroscopic data correspond to the reported data in reference 6.

**7-Chlorobenzo[*h*]quinolinyl Palladium Acetate Dimer (5)<sup>7</sup>**

To 7-chlorobenzo[*h*]quinoline (**S3**) (29 mg, 0.14 mmol, 1.0 equiv) and Pd(OAc)<sub>2</sub> (31 mg, 0.14 mmol, 1.0 equiv) in a 4 mL glass vial was added acetic acid (1.5 mL) under air. The vial was

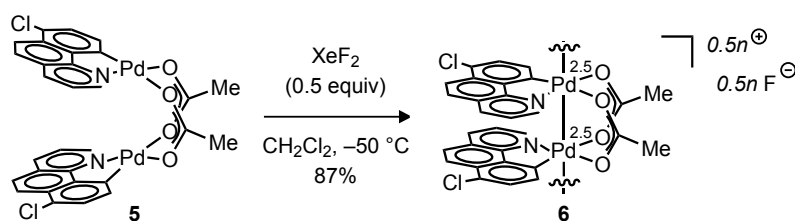
<sup>7</sup> Powers, D. C.; Benitez, D.; Tkatchouk, E.; Goddard, W. A., III; Ritter, T. *J. Am. Chem. Soc.* **2010**, *132*, 14092–14103.



sealed with a teflon-lined cap, and the reaction mixture was heated at 100 °C with stirring. After 15 minutes, the reaction mixture was cooled to 23 °C, and the solvent was removed *in vacuo*. The resulting residue was triturated with Et<sub>2</sub>O (2 × 1 mL) and then dried *in vacuo* (approx. 10 mTorr) to give 47 mg of the title compound as a yellow solid (90% yield) in a 14:1 ratio of isomers (7-chlorobenzo[*h*]quinolinylligands head to tail vs. head to head).

NMR Spectroscopy: <sup>1</sup>H-NMR (600 MHz, CDCl<sub>3</sub>, 23 °C, δ): Major Isomer : 7.92 (d, *J* = 5.1 Hz, 2H), 7.67 (d, *J* = 8.2 Hz, 2H), 7.59 (d, *J* = 8.9 Hz, 2H), 7.16 (d, *J* = 7.9 Hz, 2H), 7.14 (d, *J* = 8.9 Hz, 2H), 6.91 (d, *J* = 7.8 Hz, 2H), 6.74 (dd, *J* = 8.1 Hz, *J* = 5.1 Hz, 2H), 2.37 (s, 6H). Minor Isomer : 8.12 (d, *J* = 5.1 Hz, 2H), 7.77 (d, *J* = 7.9 Hz, 2H), 7.00 (d, *J* = 7.8 Hz, 2H), 6.96 (dd, *J* = 7.8, *J* = 5.3 Hz, 2H), 6.68 (d, *J* = 7.9 Hz, 2H). <sup>13</sup>C-NMR (125 MHz, CD<sub>2</sub>Cl<sub>2</sub>, 23 °C, δ): Major Isomer: 182.4, 152.5, 149.0, 146.6, 140.3, 135.3, 129.3, 129.2, 127.3, 126.2, 125.2, 124.1, 124.1, 120.7, 24.9. UV-VIS Spectroscopy (CH<sub>2</sub>Cl<sub>2</sub>, 23 °C): 384 nm (ε = 4.58 × 10<sup>3</sup> M<sup>-1</sup> cm<sup>-1</sup>); 291 nm (ε = 1.98 × 10<sup>4</sup> M<sup>-1</sup> cm<sup>-1</sup>). Mass Spectrometry: LRMS-FIA (m/z): calcd for [C<sub>13</sub>H<sub>7</sub>ClNPd + C<sub>2</sub>H<sub>3</sub>N]<sup>+</sup>, 358.9562. Found, 358.9580. These spectroscopic data correspond to the reported data in reference 7.

### Pd(2.5) Wire 6



7-Chlorobenzo[*h*]quinolinylligand palladium acetate dimer (**5**) (8.5 mg, 1.1 × 10<sup>-2</sup> mmol, 1.0 equiv) was dissolved in 1 mL CH<sub>2</sub>Cl<sub>2</sub> at -50 °C, and then XeF<sub>2</sub> (1.0 mg, 5.9 × 10<sup>-3</sup> mmol, 0.50 equiv) was added as a solid in one portion. The yellow solution immediately became deep red. The reaction mixture was stirred for 5 minutes, and then the solvent was evaporated *in vacuo*, maintaining a temperature of -50 °C. The residue was triturated with pentane (2 × 0.5 mL, pre-cooled to -50 °C), and then dried *in vacuo* (approx. 50 mTorr) at -50 °C to afford 7.6 mg of the title compound as a dark red-brown solid (87% yield).

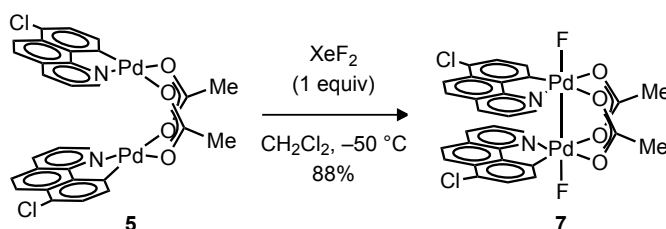
NMR Spectroscopy: <sup>1</sup>H NMR (400 MHz, CD<sub>2</sub>Cl<sub>2</sub> -25 °C, δ): 7.47 (br s), 7.29–7.08 (m), 2.31 (br s), 2.30–2.10 (br m). <sup>19</sup>F NMR (375 MHz, CD<sub>2</sub>Cl<sub>2</sub>, -25 °C, δ): 210.8 (br s). UV-VIS Spectroscopy (CH<sub>2</sub>Cl<sub>2</sub>, 23 °C): 988 nm (absorbance at this wavelength is non-linear with concentration); 380 nm (ε = 2.93 × 10<sup>3</sup> M<sup>-1</sup> cm<sup>-1</sup>). Thermal instability prevented both meaningful mass spectrometry as well as elemental analysis from being obtained. <sup>13</sup>C NMR signals were not observed.

As a note, the <sup>1</sup>H NMR spectrum for Pd(2.5) wire **6** displays very weak, broad signals that suggest a high degree of paramagnetism. This is in contrast to the <sup>1</sup>H NMR spectrum of Pd(2.5) wire **3**, which displays more well-behaved signals. Such a discrepancy suggests that alteration of

the supporting ligand scaffold may also affect the degree of electronic communication between the dipalladium units of the 1-D Pd wires in solution.

X-ray quality crystals of **6** were grown as follows: 1 mL of a solution of **6** (8 mg/mL) in CH<sub>2</sub>Cl<sub>2</sub> at –50 °C was filtered through glass wool into a 2 mL plastic vial. Pentane (1 mL, pre-cooled to –50 °C) was carefully layered on top of the solution. The vial was stored at –35 °C for 24 hours, at which point red needle crystals of the title compound were observed. X-Ray crystallographic analysis is presented in the X-ray Crystallography Data section.

**[(7-Cl-bhq)Pd(OAc)F]<sub>2</sub> (**7**)**



7-Chlorobenzo[*h*]quinolinyl palladium acetate dimer (**5**) (8.9 mg,  $1.2 \times 10^{-2}$  mmol, 1.0 equiv) was dissolved in 1 mL CH<sub>2</sub>Cl<sub>2</sub> at –50 °C. XeF<sub>2</sub> (2.0 mg,  $1.2 \times 10^{-2}$  mmol, 1.0 equiv) was added as a solid in one portion. The yellow solution immediately became deep red. After stirring for five minutes at –50 °C, the solvent was removed the solvent was evaporated *in vacuo*, maintaining a temperature of –50 °C. The residue was triturated with pentane (2 × 1 mL, pre-cooled to –50 °C), and then dried *in vacuo* (approx. 50 mTorr) at –50 °C to afford 8.3 mg of the title compound as a dark red-brown solid (88% yield).

NMR Spectroscopy: <sup>1</sup>H NMR (400 MHz, CD<sub>2</sub>Cl<sub>2</sub> –25 °C, δ): 7.98 (d, *J* = 4.4 Hz, 2H), 7.91 (d, *J* = 8.1 Hz, 2H), 7.63 (d, *J* = 9.5 Hz, 2H), 7.46 (d, *J* = 8.1 Hz, 2H), 7.32 (d, *J* = 8.8 Hz, 2H), 7.15 (d, *J* = 8.8 Hz, 2H), 7.09 (t, *J* = 6.2 Hz, 2H), 2.71 (s, 6H). <sup>19</sup>F NMR (375 MHz, CD<sub>2</sub>Cl<sub>2</sub>, –25 °C, δ): 210.8 (br s). UV-VIS Spectroscopy (CH<sub>2</sub>Cl<sub>2</sub>, 23 °C): 1002 nm (absorbance at this wavelength is non-linear with concentration); 642 nm (absorbance at this wavelength is non-linear with concentration); 468 nm (absorbance at this wavelength is non-linear with concentration); 395 nm ( $\epsilon = 2.61 \times 10^3 \text{ M}^{-1} \text{ cm}^{-1}$ ); 380 nm ( $\epsilon = 2.75 \times 10^3 \text{ M}^{-1} \text{ cm}^{-1}$ ). Thermal instability prevented both meaningful mass spectrometry as well as elemental analysis from being obtained. <sup>13</sup>C NMR signals were not observed due to low solubility at temperatures at which **7** is stable.

The broadness of the <sup>19</sup>F NMR signal observed for **7**, along with the non-linear absorbances at 468, 642, and 1002 nm, suggest that fluoride coordination to Pd is fluxional in solutions of **7**, and that Pd(III) chain species are accessible in solution. However, fluoride coordination to Pd seems to be strongly favored in the solid state, and only discrete Pd(III) dimer **7** was observed upon crystallization.

X-ray quality crystals of **7** were grown as follows: At –50 °C, 0.5 mL of a 10 mg/mL solution of **7** in CH<sub>2</sub>Cl<sub>2</sub> was filtered through glass wool into a 2.0 mL plastic vial. Pentane (1.5 mL, pre-

cooled to  $-50\text{ }^{\circ}\text{C}$ ) was carefully layered on top of the solution. The vial was stored at  $-35\text{ }^{\circ}\text{C}$  for 24 hours, at which point dark crystals were observed. X-Ray crystallographic analysis is presented in the X-ray Crystallography Data section.

## X-ray Crystallography Data

X-ray crystallographic analysis for compounds **1**, **2**, and **3**, has previously been published,<sup>8</sup> and the structures have been deposited in the CCDC: Benzo[*h*]quinolinyll Palladium Acetate Dimer (**1**), CCDC # 705005; Pd(III) Wire **2**, CCDC # 841654; Pd(2.5) Wire **3**, CCDC # 846179.

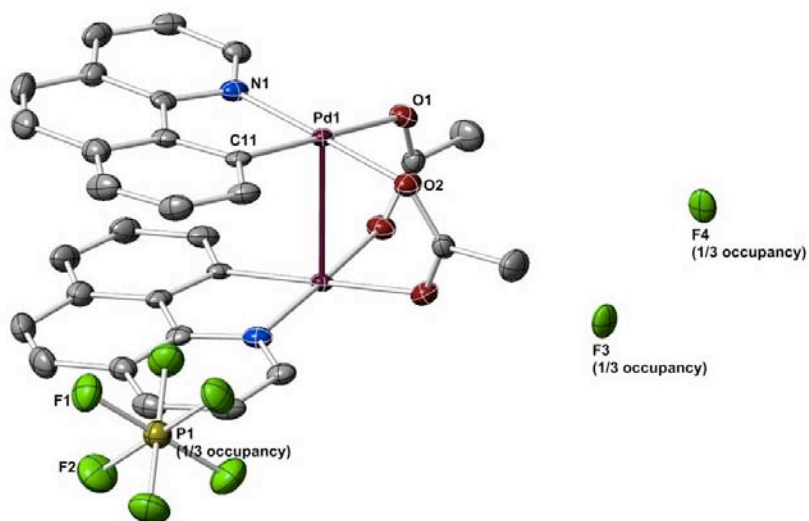
### General Procedure for X-ray Data Collection and Refinement

A crystal was mounted on a nylon loop using Paratone-N oil, and transferred to a Bruker APEX II CCD diffractometer (MoK $\alpha$  radiation,  $\lambda=0.71073\text{ }\text{\AA}$ ) equipped with an Oxford Cryosystems nitrogen flow apparatus. The sample was held at 100 K during the experiment. The collection method involved  $0.5^{\circ}$  scans in  $\omega$  at  $28^{\circ}$  in  $2\theta$ . Data integration down to  $0.82\text{ }\text{\AA}$  resolution was carried out using SAINT V7.46 A (Bruker diffractometer, 2009) with reflection spot size optimisation. Absorption corrections were made with the program SADABS (Bruker diffractometer, 2009). The structure was solved by the direct methods procedure and refined by least-squares methods against  $F^2$  using SHELXS-97 and SHELXL-97 (Sheldrick, 2008). Non-hydrogen atoms were refined anisotropically, and hydrogen atoms were allowed to ride on the respective atoms. Restraints on bond lengths and constraints of the atomic displacement parameters on each pair of disorder fragments (SADI and EADP instructions of SHELXL97), as well as the restraints of the atomic displacement parameters (SIMU/DELU instructions of SHELXL97) if necessary, have been applied for the disorder refinement. Crystal data, details of data collection and refinement, and selected geometric parameters are given for each compound in the tables below. Graphics were produced using the CystalMaker 8.6 software program (©1994-2012 CrystalMaker Software Ltd.), or with Olex2 (v1.2.2, © 2004-2013 OlexSys Ltd.).

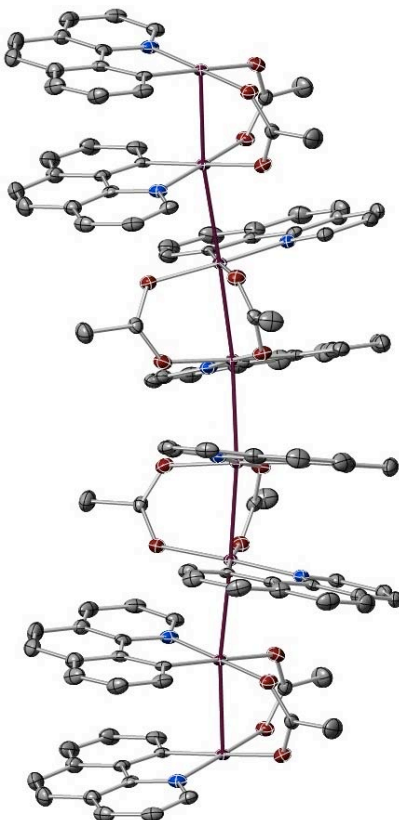
Pore diameters (data shown in Table 1) were calculated with the CystalMaker 8.6 software program, using the “Calculate Centroid” tool, and taking the average distance from all atoms that define the edge of the pore.

---

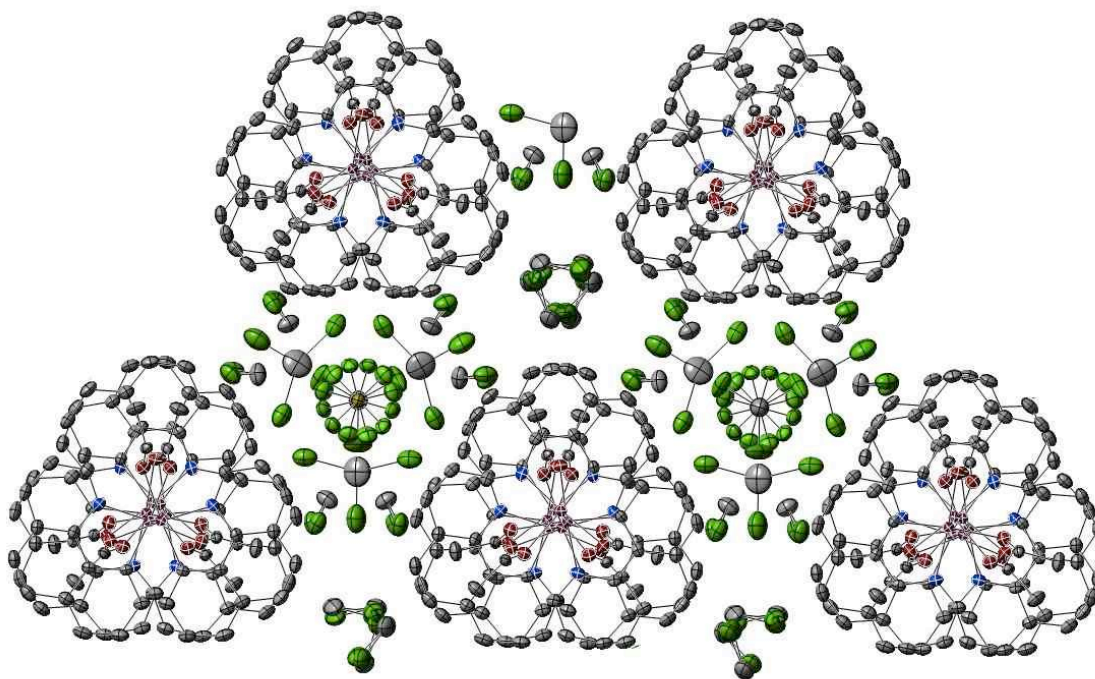
<sup>8</sup> Campbell, M. G.; Powers, D. C.; Raynaud, J.; Graham, M. J.; Xie, P.; Lee, E.; Ritter, T. *Nat. Chem.* **2011**, 3, 949–953.

**Pd(III) Wire 4 (CCDC 952240)**

X-ray structure of a single dimer of **4**, with atom labeling scheme. Thermal ellipsoids are drawn at the 50% probability level; H atoms and disordered solvent omitted for clarity.



X-ray structure of a segment of a single chain of **4**. Thermal ellipsoids are drawn at the 50% probability level; H atoms omitted for clarity.



Supramolecular structure of **4**, viewed down the crystallographic *c*-axis, showing counteranions and disordered CH<sub>2</sub>Cl<sub>2</sub> solvent molecules in the interchain channels. Thermal ellipsoids are drawn at the 50% probability level; H atoms omitted for clarity.

**Table S1. Experimental details**

	Compound <b>4</b>
<b>Crystal Data</b>	
Chemical formula	C <sub>101</sub> H <sub>88</sub> Cl <sub>22</sub> F <sub>16</sub> N <sub>6</sub> O <sub>12</sub> P <sub>2</sub> Pd <sub>6</sub>
<i>M</i> <sub>r</sub>	3362.01
Crystal system, space group	Trigonal, <i>R</i> 32
Temperature (K)	100
<i>a</i> , <i>c</i> (Å)	25.4572 (6), 16.5136 (4)
<i>V</i> (Å <sup>3</sup> )	9268.2 (4)
<i>Z</i>	3
Radiation type	Mo <i>K</i> α
μ (mm <sup>-1</sup> )	1.44

Crystal size (mm)	0.30 × 0.10 × 0.05
<b>Data Collection</b>	
Diffractometer	CCD area detector diffractometer
Absorption correction	Multi-scan <i>SADABS</i> (Sheldrick, 2009)
$T_{\min}, T_{\max}$	0.672, 0.932
No. of measured, independent and observed [ $I > 2\sigma(I)$ ] reflections	85555, 5797, 5390
$R_{\text{int}}$	0.068
$(\sin \theta/\lambda)_{\max}$ (Å <sup>-1</sup> )	0.695
<b>Refinement</b>	
$R[F^2 > 2\sigma(F^2)],$ $wR(F^2), S$	0.035, 0.080, 1.06
No. of reflections	5797
No. of parameters	275
No. of restraints	16
H-atom treatment	H-atom parameters constrained
	$w = 1/[\sigma^2(F_o^2) + (0.0402P)^2 + 32.4348P]$ where $P = (F_o^2 + 2F_c^2)/3$
$\Delta\rho_{\max}, \Delta\rho_{\min}$ (e Å <sup>-3</sup> )	1.68, -0.91
Absolute structure	Flack H D (1983), Acta Cryst. A39, 876-881
Flack parameter	-0.03 (3)

Computer programs: *APEX2* v2009.3.0 (Bruker-AXS, 2009), *SAINT* 7.46A (Bruker-AXS, 2009), *SHELXS97* (Sheldrick, 2008), *SHELXL97* (Sheldrick, 2008), Bruker *SHELXTL*.

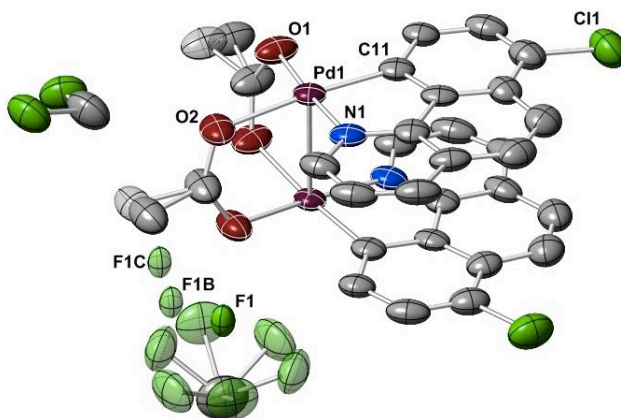
**Table S2. Selected geometric parameters (Å, °)**

Pd1—C11	1.992 (3)	C3—C4	1.398 (5)
Pd1—N1	2.020 (3)	C4—C13	1.399 (5)
Pd1—O2 <sup>i</sup>	2.067 (2)	C4—C5	1.441 (6)
Pd1—O1	2.090 (2)	C5—C6	1.356 (6)
Pd1—Pd1 <sup>i</sup>	2.7112 (4)	C6—C7	1.434 (6)
Pd1—Pd1 <sup>ii</sup>	2.8428 (4)	C7—C8	1.405 (6)
O1—C14	1.258 (4)	C7—C12	1.412 (5)
O2—C14	1.263 (4)	C8—C9	1.379 (6)
O2—Pd1 <sup>i</sup>	2.067 (2)	C9—C10	1.415 (6)
N1—C1	1.342 (5)	C10—C11	1.354 (5)
N1—C13	1.377 (4)	C11—C12	1.389 (5)
C1—C2	1.392 (5)	C12—C13	1.424 (5)
C2—C3	1.391 (6)	C14—C15	1.504 (5)
C11—Pd1—N1	82.77 (13)	C3—C4—C13	117.3 (3)
C11—Pd1—O2 <sup>i</sup>	93.15 (12)	C3—C4—C5	125.4 (3)
N1—Pd1—O2 <sup>i</sup>	175.65 (11)	C13—C4—C5	117.3 (3)
C11—Pd1—O1	175.18 (12)	C6—C5—C4	121.6 (4)
N1—Pd1—O1	93.14 (11)	C5—C6—C7	121.8 (4)
O2 <sup>i</sup> —Pd1—O1	91.00 (10)	C8—C7—C12	116.8 (3)
C11—Pd1—Pd1 <sup>i</sup>	95.45 (8)	C8—C7—C6	125.6 (4)
N1—Pd1—Pd1 <sup>i</sup>	98.77 (8)	C12—C7—C6	117.6 (3)
O2 <sup>i</sup> —Pd1—Pd1 <sup>i</sup>	83.08 (7)	C9—C8—C7	120.5 (3)
O1—Pd1—Pd1 <sup>i</sup>	82.60 (6)	C8—C9—C10	120.7 (3)
C11—Pd1—Pd1 <sup>ii</sup>	91.88 (8)	C11—C10—C9	120.1 (4)
N1—Pd1—Pd1 <sup>ii</sup>	84.69 (8)	C10—C11—C12	119.2 (3)
O2 <sup>i</sup> —Pd1—Pd1 <sup>ii</sup>	93.96 (7)	C10—C11—Pd1	128.7 (3)
O1—Pd1—Pd1 <sup>ii</sup>	90.29 (6)	C12—C11—Pd1	112.0 (2)
Pd1 <sup>i</sup> —Pd1—Pd1 <sup>ii</sup>	172.233 (5)	C11—C12—C7	122.7 (3)

C14—O1—Pd1	122.7 (2)	C11—C12—C13	117.0 (3)
C14—O2—Pd1 <sup>i</sup>	122.8 (2)	C7—C12—C13	120.3 (3)
C1—N1—C13	119.0 (3)	N1—C13—C4	122.8 (3)
C1—N1—Pd1	128.7 (2)	N1—C13—C12	115.7 (3)
C13—N1—Pd1	112.3 (2)	C4—C13—C12	121.5 (3)
N1—C1—C2	120.9 (3)	O1—C14—O2	125.4 (3)
C3—C2—C1	120.5 (3)	O1—C14—C15	117.6 (3)
C2—C3—C4	119.5 (3)	O2—C14—C15	117.1 (3)

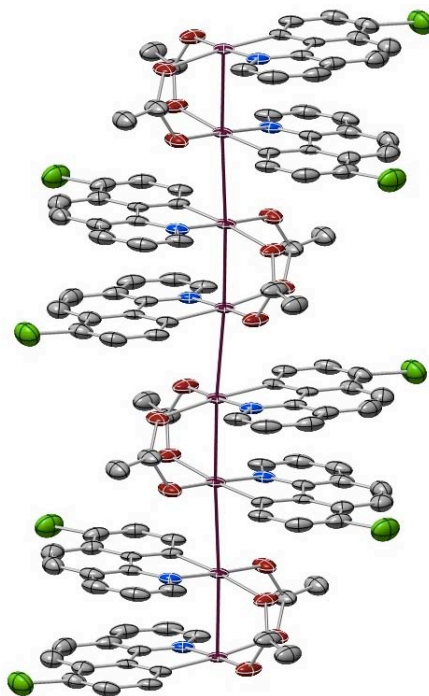
Symmetry code(s): (i)  $-x+2/3, -x+y+1/3, -z+4/3$ ; (ii)  $y, x, -z+1$ .

**Pd(2.5) Wire 6 (CCDC 952241)**

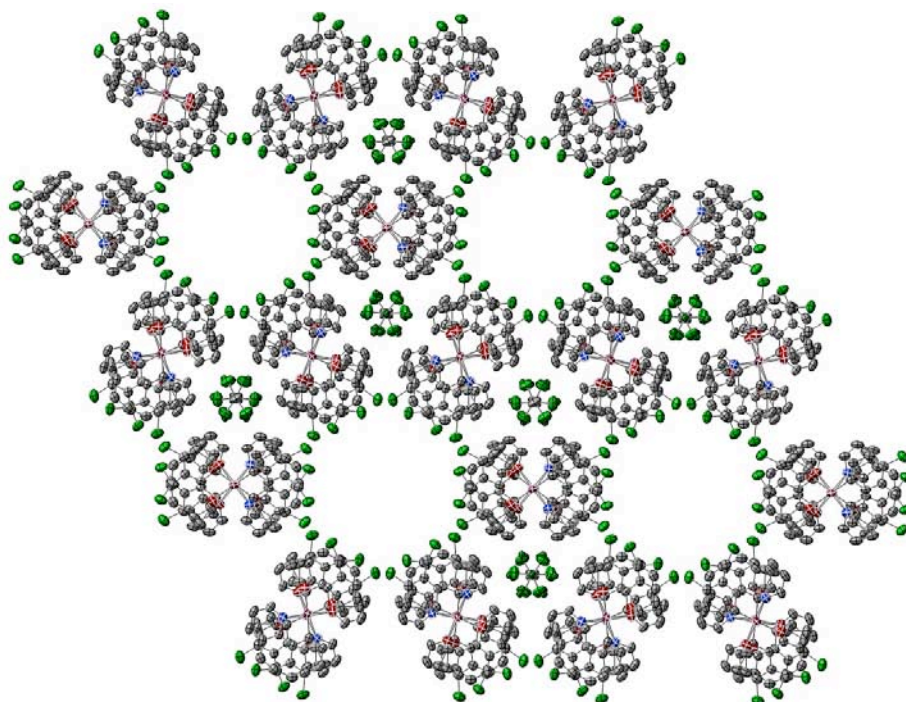


X-ray structure of a single dimer of **6**, with atom labeling scheme. Thermal ellipsoids are drawn at the 50% probability level; H atoms omitted for clarity. The disorder model is depicted using transparent ellipsoids.

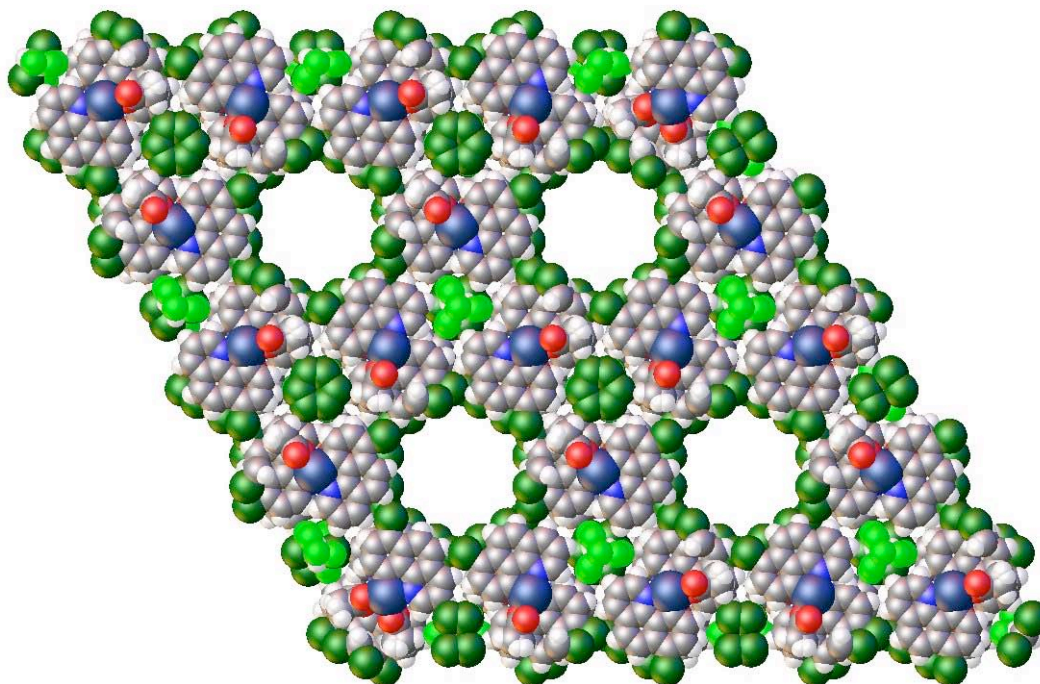




X-ray structure of a segment of a single chain of **6**. Thermal ellipsoids are drawn at the 50% probability level; H atoms and disorder omitted for clarity.



Supramolecular structure of **6**, viewed down the crystallographic *c*-axis, showing counteranions and disordered CH<sub>2</sub>Cl<sub>2</sub> solvent molecules in the interchain channels. Thermal ellipsoids are drawn at the 50% probability level; H atoms omitted for clarity.



Space-filling projection of **6**, viewed down the crystallographic *c*-axis, showing empty pores lined by the chloride substituents of the cyclometallated ligands.

**Table S3. Experimental details**

	Compound <b>6</b>
<b>Crystal Data</b>	
Chemical formula	C <sub>30.58</sub> H <sub>21.17</sub> Cl <sub>3.17</sub> FN <sub>2</sub> O <sub>4</sub> Pd <sub>2</sub>
<i>M</i> <sub>r</sub>	824.72
Crystal system, space group	Trigonal, <i>P</i> $\bar{3}$ <i>c</i> 1
Temperature (K)	100
<i>a</i> , <i>c</i> (Å)	23.8680 (15), 11.2498 (7)
<i>V</i> (Å <sup>3</sup> )	5550.2 (6)
<i>Z</i>	6
Radiation type	Mo <i>K</i> α
μ (mm <sup>-1</sup> )	1.24
Crystal size (mm)	0.30 × 0.20 × 0.10

<b>Data Collection</b>	
Diffractometer	CCD area detector diffractometer
Absorption correction	Multi-scan <i>SADABS</i> (Sheldrick, 2009)
$T_{\min}, T_{\max}$	0.708, 0.886
No. of measured, independent and observed [ $I > 2\sigma(I)$ ] reflections	69099, 3280, 2563
$R_{\text{int}}$	0.045
$(\sin \theta/\lambda)_{\text{max}}$ ( $\text{\AA}^{-1}$ )	0.596
<b>Refinement</b>	
$R[F^2 > 2\sigma(F^2)]$ , $wR(F^2)$ , $S$	0.053, 0.203, 1.08
No. of reflections	3280
No. of parameters	222
No. of restraints	12
H-atom treatment	H-atom parameters constrained
	$w = 1/[\sigma^2(F_o^2) + (0.1032P)^2 + 28.9902P]$ where $P = (F_o^2 + 2F_c^2)/3$
$\Delta\rho_{\text{max}}, \Delta\rho_{\text{min}}$ ( $\text{e \AA}^{-3}$ )	1.25, -1.75

Computer programs: *APEX2* v2009.3.0 (Bruker-AXS, 2009), *SAINT* 7.46A (Bruker-AXS, 2009), *SHELXS97* (Sheldrick, 2008), *SHELXL97* (Sheldrick, 2008), Bruker *SHELXTL*.

**Table S4. Selected geometric parameters ( $\text{\AA}$ ,  $^\circ$ )**

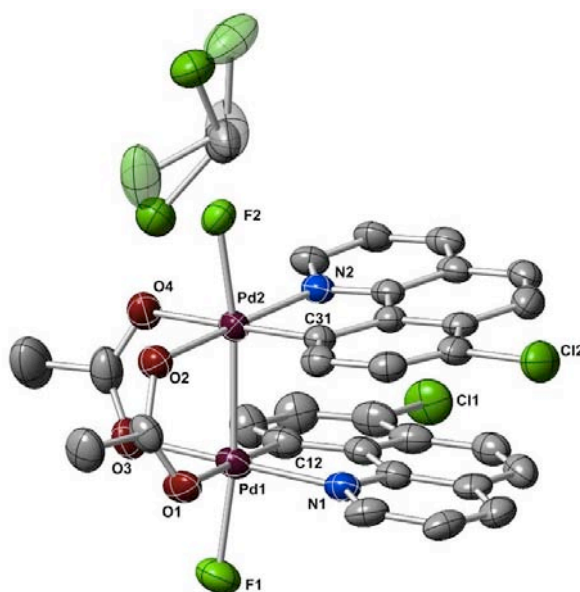
C1—N1	1.328 (8)	C11—C12	1.416 (9)
C1—C2	1.389 (11)	C11—Pd1	1.960 (7)
C2—C3	1.364 (12)	C12—C13	1.434 (9)
C3—C4	1.417 (10)	C13—N1	1.357 (9)
C4—C13	1.401 (10)	C14—O2	1.255 (8)

C4—C5	1.427 (11)	C14—O1	1.267 (8)
C5—C6	1.341 (11)	C14—C15	1.528 (12)
C6—C7	1.428 (10)	C14—C15B	1.531 (18)
C7—C12	1.395 (9)	N1—Pd1	2.025 (6)
C7—C8	1.415 (10)	O1—Pd1	2.029 (5)
C8—C9	1.372 (11)	O2—Pd1 <sup>i</sup>	2.128 (5)
C8—C11	1.744 (8)	Pd1—O2 <sup>i</sup>	2.128 (5)
C9—C10	1.398 (10)	Pd1—Pd1 <sup>i</sup>	2.7271 (8)
C10—C11	1.370 (9)	Pd1—Pd1 <sup>ii</sup>	2.9053 (8)
N1—C1—C2	122.0 (7)	O2—C14—C15	119.2 (8)
C3—C2—C1	120.3 (7)	O1—C14—C15	114.7 (8)
C2—C3—C4	119.6 (7)	O2—C14—C15B	116.6 (18)
C13—C4—C3	116.1 (7)	O1—C14—C15B	114.8 (16)
C13—C4—C5	117.6 (6)	C15—C14—C15B	25.6 (17)
C3—C4—C5	126.2 (7)	C1—N1—C13	118.3 (6)
C6—C5—C4	122.1 (7)	C1—N1—Pd1	129.0 (5)
C5—C6—C7	121.1 (7)	C13—N1—Pd1	112.6 (4)
C12—C7—C8	114.9 (6)	C14—O1—Pd1	122.4 (5)
C12—C7—C6	119.0 (6)	C14—O2—Pd1 <sup>i</sup>	122.0 (5)
C8—C7—C6	126.1 (7)	C11—Pd1—N1	83.2 (2)
C9—C8—C7	121.4 (7)	C11—Pd1—O1	93.0 (3)
C9—C8—C11	119.3 (6)	N1—Pd1—O1	176.1 (2)
C7—C8—C11	119.2 (6)	C11—Pd1—O2 <sup>i</sup>	175.0 (2)
C8—C9—C10	122.0 (6)	N1—Pd1—O2 <sup>i</sup>	93.5 (2)
C11—C10—C9	119.2 (7)	O1—Pd1—O2 <sup>i</sup>	90.4 (2)
C10—C11—C12	118.1 (6)	C11—Pd1—Pd1 <sup>i</sup>	96.23 (16)
C10—C11—Pd1	129.7 (5)	N1—Pd1—Pd1 <sup>i</sup>	96.71 (13)
C12—C11—Pd1	112.0 (5)	O1—Pd1—Pd1 <sup>i</sup>	84.34 (12)

C7—C12—C11	124.4 (6)	O2 <sup>i</sup> —Pd1—Pd1 <sup>i</sup>	80.40 (11)
C7—C12—C13	119.3 (6)	C11—Pd1—Pd1 <sup>ii</sup>	79.07 (16)
C11—C12—C13	116.2 (6)	N1—Pd1—Pd1 <sup>ii</sup>	83.86 (13)
N1—C13—C4	123.7 (6)	O1—Pd1—Pd1 <sup>ii</sup>	94.78 (12)
N1—C13—C12	115.5 (6)	O2 <sup>i</sup> —Pd1—Pd1 <sup>ii</sup>	104.36 (12)
C4—C13—C12	120.8 (6)	Pd1 <sup>i</sup> —Pd1—Pd1 <sup>ii</sup>	175.18 (3)
O2—C14—O1	125.6 (7)		

Symmetry code(s): (i)  $y, x, -z+1/2$ ; (ii)  $-x+1, -y+1, -z+1$ .

### Pd(III) Fluoride Dimer 7 (CCDC 952242)



X-ray structure of **7** with atom labeling scheme. Thermal ellipsoids are drawn at the 50% probability level; H atoms omitted for clarity. The disorder model is depicted using transparent ellipsoids.

**Table S5. Experimental details**

	Compound <b>7</b>
<b>Crystal Data</b>	
Chemical formula	C <sub>31</sub> H <sub>22</sub> Cl <sub>4</sub> F <sub>2</sub> N <sub>2</sub> O <sub>4</sub> Pd <sub>2</sub>
$M_r$	879.11
Crystal system,	Triclinic, $P\bar{1}$

space group	
Temperature (K)	100
$a, b, c$ (Å)	11.889 (5), 12.979 (6), 13.683 (6)
$\alpha, \beta, \gamma$ (°)	96.574 (5), 98.900 (6), 91.797 (6)
$V$ (Å <sup>3</sup> )	2069.8 (15)
$Z$	2
Radiation type	Mo $K\alpha$
$\mu$ (mm <sup>-1</sup> )	1.17
Crystal size (mm)	0.26 × 0.12 × 0.08
<b>Data Collection</b>	
Diffractometer	CCD area detector diffractometer
Absorption correction	Multi-scan <i>SADABS</i> (Sheldrick, 2009)
$T_{\min}, T_{\max}$	0.751, 0.912
No. of measured, independent and observed [ $I > 2\sigma(I)$ ] reflections	19066, 7740, 5280
$R_{\text{int}}$	0.049
$(\sin \theta/\lambda)_{\text{max}}$ (Å <sup>-1</sup> )	0.613
<b>Refinement</b>	
$R[F^2 > 2\sigma(F^2)],$ $wR(F^2), S$	0.053, 0.127, 1.03
No. of reflections	7740
No. of parameters	436
No. of restraints	32
H-atom treatment	H-atom parameters constrained
$\Delta\rho_{\text{max}}, \Delta\rho_{\text{min}}$ (e Å <sup>-3</sup> )	1.67, -0.82

Computer programs: *APEX2* v2009.3.0 (Bruker-AXS, 2009), *SAINT* 7.46A (Bruker-AXS, 2009), *SHELXS97* (Sheldrick, 2008), *SHELXL97* (Sheldrick, 2008), Bruker *SHELXTL*.

**Table S6. Selected geometric parameters (Å, °)**

Pd1—C11	1.983 (5)	C4—C13	1.401 (7)
Pd1—O3	2.008 (4)	C4—C5	1.435 (7)
Pd1—N1	2.026 (4)	C5—C6	1.348 (8)
Pd1—F1	2.065 (3)	C6—C7	1.422 (8)
Pd1—O1	2.146 (4)	C7—C8	1.409 (8)
Pd1—Pd2	2.5227 (12)	C7—C12	1.412 (7)
Pd2—C31	1.981 (5)	C8—C9	1.367 (8)
Pd2—O2	2.010 (4)	C9—C10	1.428 (8)
Pd2—N2	2.027 (4)	C10—C11	1.359 (8)
Pd2—F2	2.048 (3)	C11—C12	1.405 (7)
Pd2—O4	2.139 (4)	C12—C13	1.413 (7)
C11—C28	1.746 (5)	C21—C22	1.393 (7)
C12—C8	1.733 (6)	C22—C23	1.370 (7)
O1—C41	1.245 (6)	C23—C24	1.412 (8)
O2—C41	1.290 (6)	C24—C25	1.420 (7)
O3—C43	1.275 (7)	C25—C26	1.356 (8)
O4—C43	1.264 (7)	C26—C27	1.435 (7)
N1—C1	1.319 (7)	C27—C32	1.406 (7)
N1—C13	1.362 (6)	C27—C28	1.430 (8)
N2—C21	1.334 (7)	C28—C29	1.355 (7)
N2—C33	1.343 (6)	C29—C30	1.410 (7)
C1—C2	1.392 (8)	C30—C31	1.368 (7)
C2—C3	1.368 (8)	C31—C32	1.420 (7)
C3—C4	1.406 (8)	C41—C42	1.487 (7)
C33—C32	1.406 (7)	C43—C44	1.485 (8)
C33—C24	1.410 (7)		

C11—Pd1—O3	92.9 (2)	C3—C4—C5	125.9 (5)
C11—Pd1—N1	82.6 (2)	C6—C5—C4	121.5 (5)
O3—Pd1—N1	175.41 (17)	C5—C6—C7	121.9 (5)
C11—Pd1—F1	90.43 (18)	C8—C7—C12	115.4 (5)
O3—Pd1—F1	89.64 (15)	C8—C7—C6	126.4 (5)
N1—Pd1—F1	89.60 (15)	C12—C7—C6	118.1 (5)
C11—Pd1—O1	178.71 (19)	C9—C8—C7	121.6 (5)
O3—Pd1—O1	88.07 (16)	C9—C8—C12	118.9 (5)
N1—Pd1—O1	96.44 (16)	C7—C8—C12	119.5 (5)
F1—Pd1—O1	88.69 (14)	C8—C9—C10	122.0 (6)
C11—Pd1—Pd2	96.75 (15)	C11—C10—C9	117.5 (5)
O3—Pd1—Pd2	85.13 (12)	C10—C11—C12	120.5 (5)
N1—Pd1—Pd2	96.17 (11)	C10—C11—Pd1	128.0 (4)
F1—Pd1—Pd2	171.31 (10)	C12—C11—Pd1	111.4 (4)
O1—Pd1—Pd2	84.21 (10)	C11—C12—C7	122.8 (5)
C31—Pd2—O2	93.52 (18)	C11—C12—C13	117.7 (5)
C31—Pd2—N2	82.83 (19)	C7—C12—C13	119.5 (5)
O2—Pd2—N2	176.21 (16)	N1—C13—C4	122.8 (5)
C31—Pd2—F2	88.64 (16)	N1—C13—C12	115.2 (5)
O2—Pd2—F2	88.16 (13)	C4—C13—C12	122.0 (5)
N2—Pd2—F2	90.73 (14)	N2—C21—C22	120.0 (5)
C31—Pd2—O4	178.04 (17)	C23—C22—C21	121.0 (5)
O2—Pd2—O4	88.43 (15)	C22—C23—C24	119.6 (5)
N2—Pd2—O4	95.22 (16)	C33—C24—C23	116.2 (5)
F2—Pd2—O4	91.44 (14)	C33—C24—C25	117.4 (5)
C31—Pd2—Pd1	95.95 (13)	C23—C24—C25	126.4 (5)
O2—Pd2—Pd1	85.19 (10)	C26—C25—C24	121.9 (5)
N2—Pd2—Pd1	96.17 (11)	C25—C26—C27	121.2 (5)



F2—Pd2—Pd1	172.13 (8)	C32—C27—C28	115.6 (5)
O4—Pd2—Pd1	84.19 (11)	C32—C27—C26	117.8 (5)
C41—O1—Pd1	116.3 (3)	C28—C27—C26	126.6 (5)
C41—O2—Pd2	122.4 (3)	C29—C28—C27	122.2 (5)
C43—O3—Pd1	122.6 (4)	C29—C28—C11	119.7 (4)
C43—O4—Pd2	116.4 (4)	C27—C28—C11	118.2 (4)
C1—N1—C13	119.1 (5)	C28—C29—C30	121.2 (5)
C1—N1—Pd1	127.9 (4)	C31—C30—C29	119.0 (5)
C13—N1—Pd1	113.0 (3)	C30—C31—C32	120.0 (5)
C21—N2—C33	120.4 (4)	C30—C31—Pd2	129.4 (4)
C21—N2—Pd2	126.6 (4)	C32—C31—Pd2	110.6 (4)
C33—N2—Pd2	113.0 (3)	C33—C32—C27	120.5 (5)
N1—C1—C2	121.1 (5)	C33—C32—C31	117.6 (5)
C3—C2—C1	121.1 (5)	C27—C32—C31	121.9 (5)
C2—C3—C4	118.8 (5)	O1—C41—O2	124.3 (5)
N2—C33—C32	115.9 (4)	O1—C41—C42	120.3 (5)
N2—C33—C24	122.8 (5)	O2—C41—C42	115.3 (5)
C32—C33—C24	121.2 (5)	O4—C43—O3	124.2 (5)
C13—C4—C3	117.1 (5)	O4—C43—C44	120.0 (6)
C13—C4—C5	117.0 (5)	O3—C43—C44	115.8 (6)

## DFT Calculations

Density functional theory (DFT) calculations were performed using Gaussian09<sup>9</sup> at the Odyssey cluster at Harvard University. Geometry optimization was carried out using the atomic coordinates from the crystal structure of **7** as a starting point. The unrestricted wave function was used for ground state optimizations. BS I includes SDD quasirelativistic pseudopotentials on Pd (28) and Cl (10) with basis sets (Pd: (8s7p6d)/[6s5p3d]<sup>10</sup>; Cl: (4s5p)/[2s3p]<sup>11</sup>) extended by polarization functions (Pd: f, 1.472<sup>12</sup>; Cl: d, 0.640<sup>13</sup>), and 6-31G(d,p)<sup>14</sup> on H, C, O, N, F. All geometry optimizations were performed using the B3PW91 functional with the BS I basis set. Molecular orbitals were generated using an isosurface value of 0.03 with B3PW91/BS I. Analysis of the simulated UV-vis spectrum of **7** was carried out using Chemissian.<sup>15</sup>

---

<sup>9</sup> Frisch, M. J.; Trucks, G. W.; Schlegel, H. B.; Scuseria, G. E.; Robb, M. A.; Cheeseman, J. R.; Scalmani, G.; Barone, V.; Mennucci, B.; Petersson, G. A.; Nakatsuji, H.; Caricato, M.; Li, X.; Hratchian, H. P.; Izmaylov, A. F.; Bloino, J.; Zheng, G.; Sonnenberg, J. L.; Hada, M.; Ehara, M.; Toyota, K.; Fukuda, R.; Hasegawa, J.; Ishida, M.; Nakajima, T.; Honda, Y.; Kitao, O.; Nakai, H.; Vreven, T.; Montgomery, J. J.; Peralta, J. E.; Ogliaro, F.; Bearpark, M.; Heyd, J. J.; Brothers, E.; Kudin, K. N.; Staroverov, V. N.; Normand, J.; Raghavachari, K.; Rendell, A.; Burant, J. C.; Iyengar, S. S.; Cossi, J. M.; Rega, N.; Millam, J. M.; Klene, M.; Knox, J. E.; Cross, J. B.; Bakken, V.; Adam, C.; Jaramillo, J.; Gomperts, R.; Stratmann, R. E.; Yazyev, O.; Austin, A. J.; Cammi, R.; Pomelli, C.; Ochterski, J. W.; Martin, R. L.; Morokuma, K.; Zakrzewski, V. G.; Voth, G. A.; Salvador, P.; Dannenberg, J. J.; Dapprich, S.; Daniels, A. D.; Farkas, O.; Foresman, J. B.; Ortiz, J. V.; Cioslowski, J.; Fox, D. J. *Gaussian 09, Revision A.02*; Gaussian, Inc.: Wallingford CT, 2009.

<sup>10</sup> (a) Andrae, D.; Häussermann, U.; Dolg, M.; Stoll, H.; Preuss, H. *Theor. Chim. Acta* **1990**, *77*, 123-141. (b) Andrae, D.; Häussermann, U.; Dolg, M.; Stoll, H.; Preuss, H. *Theor. Chim. Acta* **1991**, *78*, 247-266.

<sup>11</sup> Bergner, A.; Dolg, M.; Küchle, W.; Stoll, H.; Preuss, H. *Mol. Phys.* **1993**, *30*, 1431-1441.

<sup>12</sup> Ehlers, A. W.; Böhme, M.; Dapprich, S.; Gobbi, A.; Höllwarth, A.; Jonas, V.; Köhler, K. F.; Stegmann, R.; Veldkamp, A.; Frenking, G. *Chem. Phys. Lett.* **1993**, *208*, 111-114.

<sup>13</sup> Höllwarth, A.; Böhme, M.; Dapprich, S.; Ehlers, A. W.; Gobbi, A.; Jonas, V.; Köhler, K. F.; Stegmann, R.; Veldkamp, A.; Frenking, G. *Chem. Phys. Lett.* **1993**, *208*, 237-240.

<sup>14</sup> Hariharan, P. C.; Pople, J. A. *Theor. Chim. Acta* **1973**, *28*, 213-222.

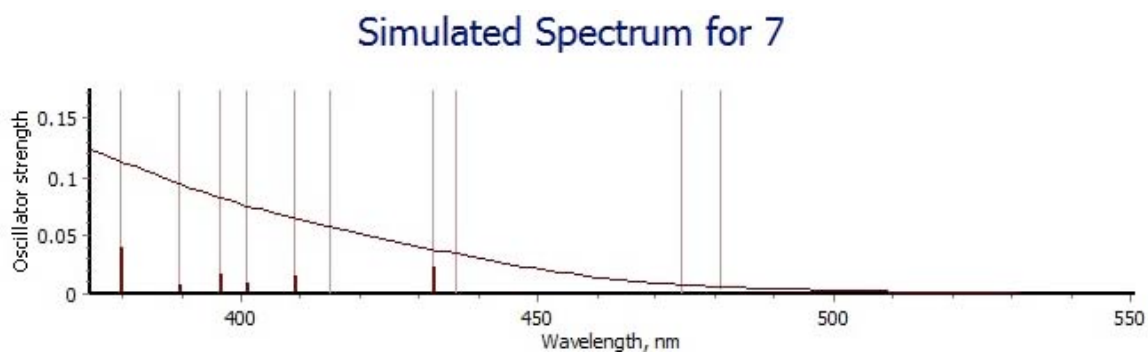
<sup>15</sup> *Chemissian*, Version 3.3; © Skripnikov Leonid 2005-2012; www.chemissian.com

**Cartesian Coordinates for the Optimized Structure of 7**

<b>Atom</b>	<b>X</b>	<b>Y</b>	<b>Z</b>
Pd	0.70727	1.44218	-1.08123
Cl	5.13092	-3.15394	0.26072
Cl	-5.13307	-3.15025	-0.26095
F	-1.76326	1.67228	2.77772
F	1.76432	1.67102	-2.77783
O	0.86252	2.71589	1.8201
O	1.6253	3.05484	-0.27279
O	-1.62314	3.05607	0.27283
O	-0.86081	2.7163	-1.82009
N	0.05407	-0.21169	1.95536
N	-0.05426	-0.21173	-1.95524
C	1.10479	-0.26113	2.76328
C	1.46135	-1.45284	3.41146
C	0.70163	-2.59359	3.22184
C	0.73034	-1.3066	-1.78769
C	-0.44058	-2.54069	2.39943
C	-1.34659	-3.62484	2.15188
C	-2.46651	-3.45513	1.38911
C	-2.7931	-2.18582	0.80392
C	-3.96116	-1.8868	0.0685
C	-4.21701	-0.60459	-0.38236
C	-3.30714	0.44817	-0.15041
C	-2.12333	0.19109	0.50918
C	-1.89397	-1.11017	0.99898
C	-0.73139	-1.30597	1.78787
C	-1.10502	-0.26039	-2.76317
C	-1.46253	-1.45186	-3.41124
C	-0.70373	-2.59321	-3.22152
C	0.43854	-2.54115	-2.39914
C	1.34373	-3.62597	-2.15152
C	2.46386	-3.45702	-1.38888
C	2.7915	-2.1879	-0.80389
C	3.95991	-1.88965	-0.06869
C	4.2168	-0.60757	0.38193
C	3.30766	0.44584	0.15001
C	2.12354	0.18954	-0.50932
C	1.89314	-1.11161	-0.99893
C	1.54056	3.3443	0.9688
C	2.31697	4.55553	1.41805
C	-1.53809	3.3455	-0.96875

C	-2.31303	4.55769	-1.41791
H	1.657	0.66317	2.88558
H	2.33411	-1.46041	4.05479
H	0.97075	-3.52363	3.71539
H	-1.13497	-4.59158	2.60015
H	-3.1455	-4.28631	1.23084
H	-5.14328	-0.40629	-0.91227
H	-3.56426	1.44951	-0.47628
H	-1.65648	0.66436	-2.88553
H	-2.3353	-1.45879	-4.05457
H	-0.97361	-3.52308	-3.71498
H	1.13132	-4.5926	-2.59965
H	3.14222	-4.28872	-1.23059
H	5.14331	-0.40988	0.91164
H	3.5656	1.44704	0.47565
H	3.07017	4.83638	0.68182
H	2.77483	4.36152	2.39041
H	1.61433	5.3849	1.54712
H	-1.6095	5.38649	-1.54575
H	-3.06662	4.83877	-0.68216
H	-2.77016	4.36476	-2.39083

### Simulated UV-vis Spectrum for 7



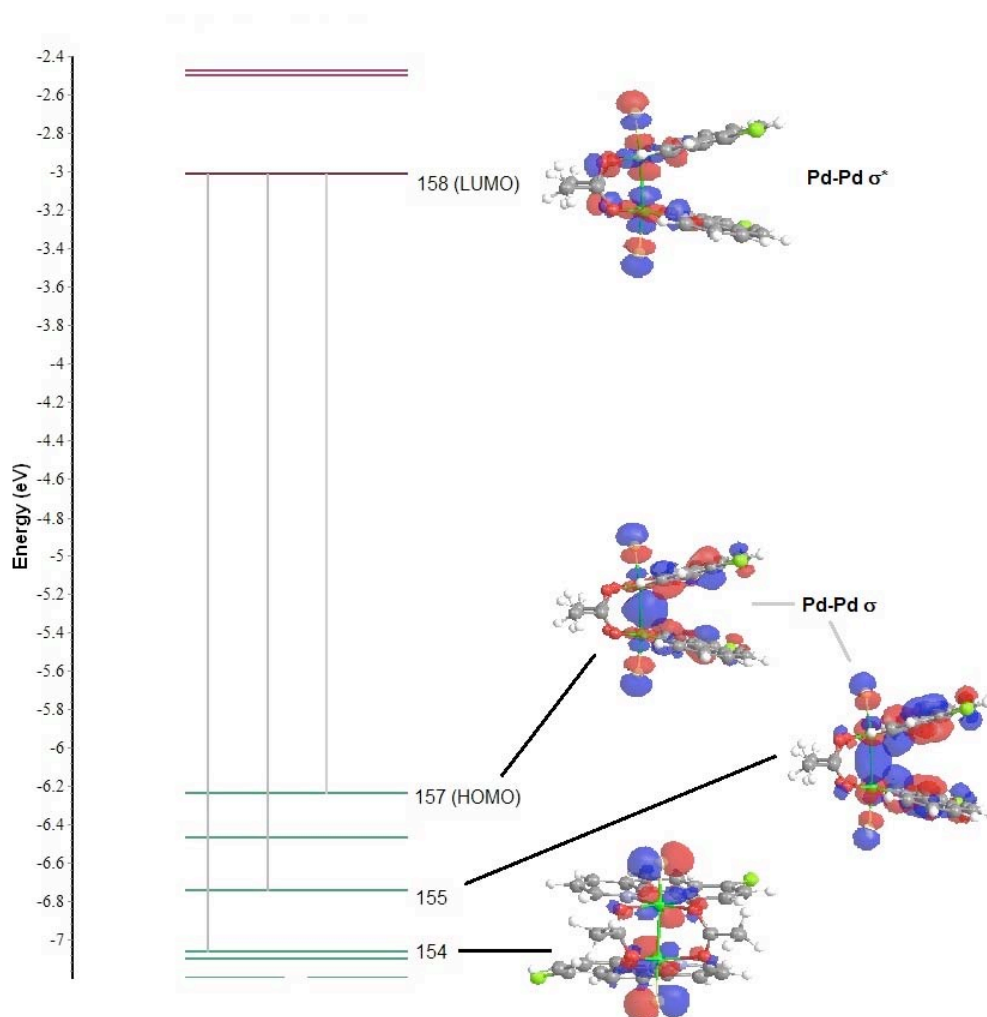
Shown below are the electronic transitions that contribute to the predicted absorbances at 481 nm and 432 nm (the predicted absorbances at 474 and 436 nm have oscillator strengths  $\leq 0.0002$ , and are therefore not analyzed):

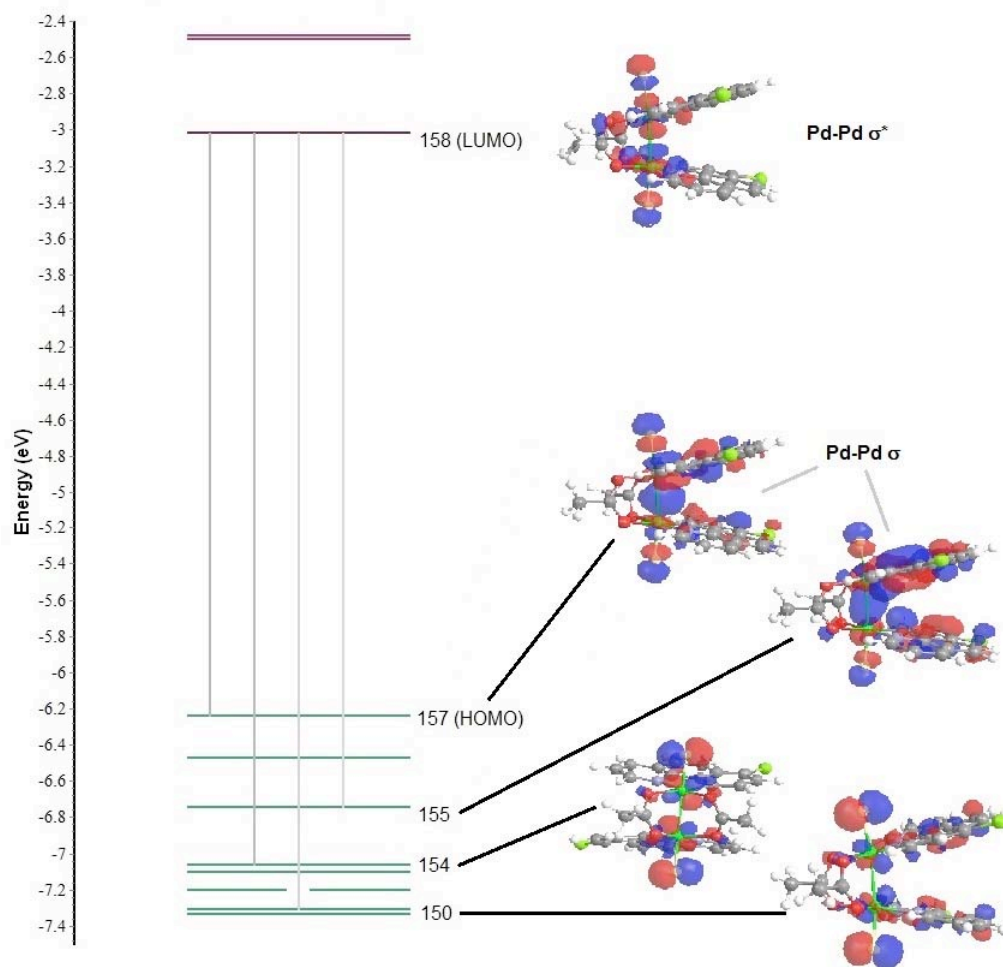
Excited State 1:	Singlet-A	2.5773 eV	481.06 nm	f=0.0034	$\langle S^2 \rangle = 0.000$
154 -> 158	0.44020				
155 -> 158	0.43387				
157 -> 158	-0.30188				

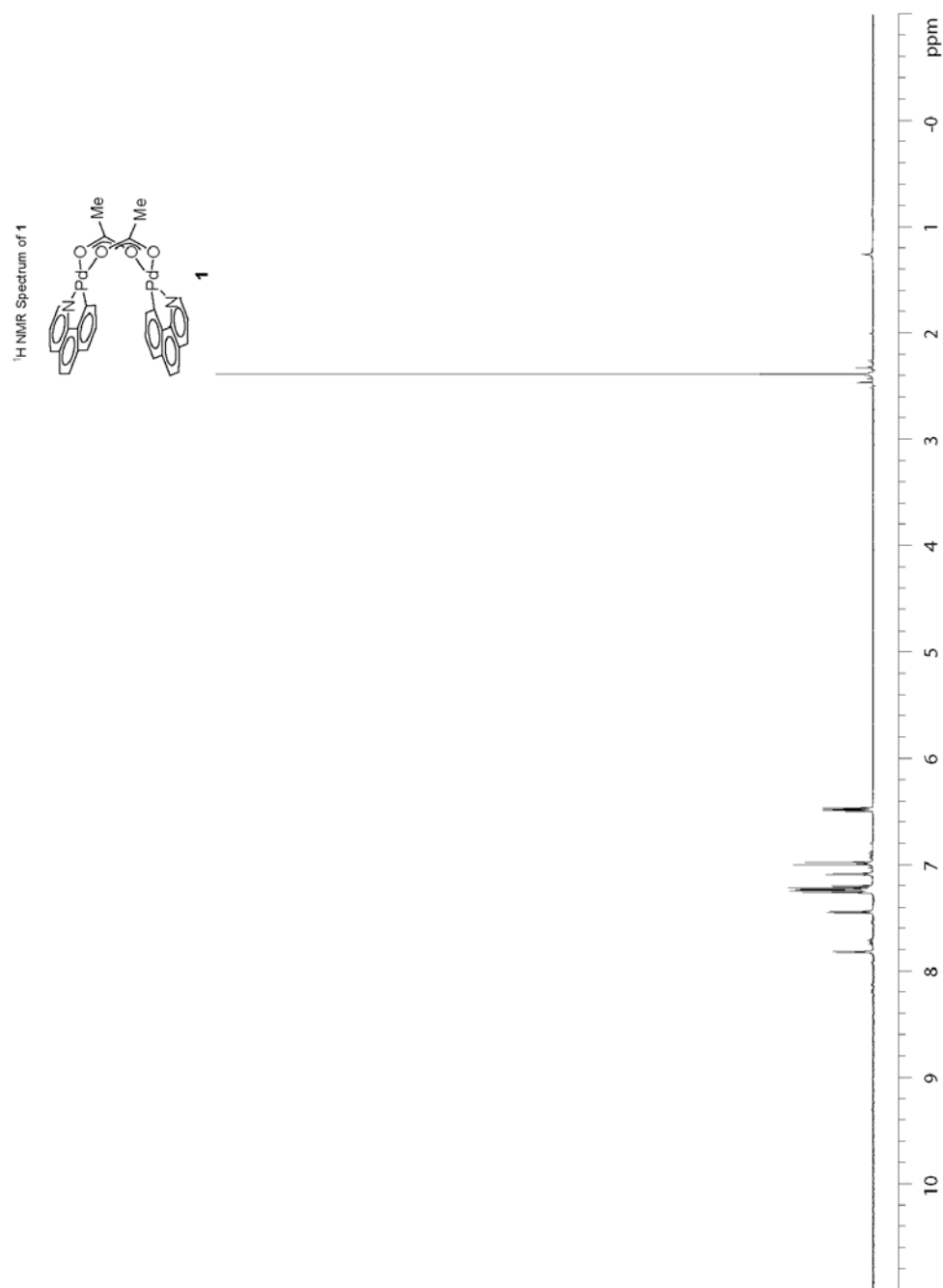
Excited State	4:	Singlet-A	2.8682 eV	432.27 nm	f=0.0223	$\langle S^2 \rangle = 0.000$
150 ->158			0.20751			
154 ->158			0.43745			
155 ->158			-0.16198			
157 ->158			0.44633			

As shown below, the predicted absorbances at 481 and 432 nm are largely due to Pd–Pd  $\sigma \rightarrow \sigma^*$  transitions in Pd(III) dimer **7**; therefore, we believe that the observation of absorbances at both 468 and 1002 nm in the experimental UV-vis/NIR spectrum of **7** is likely due to an equilibrium between 1-D Pd(III) chains and discrete dimer **7**.

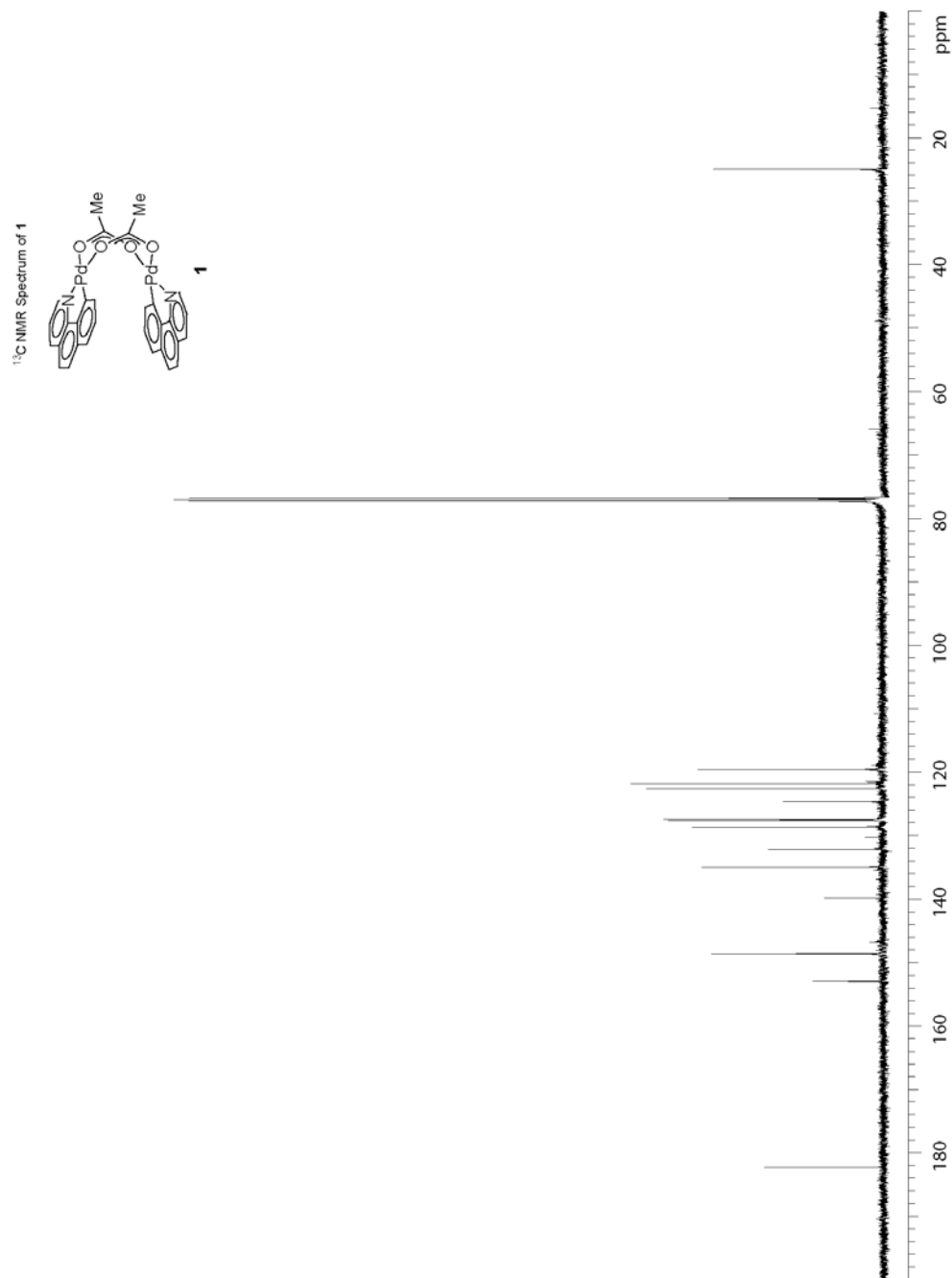
#### 481 nm:



**432 nm:**

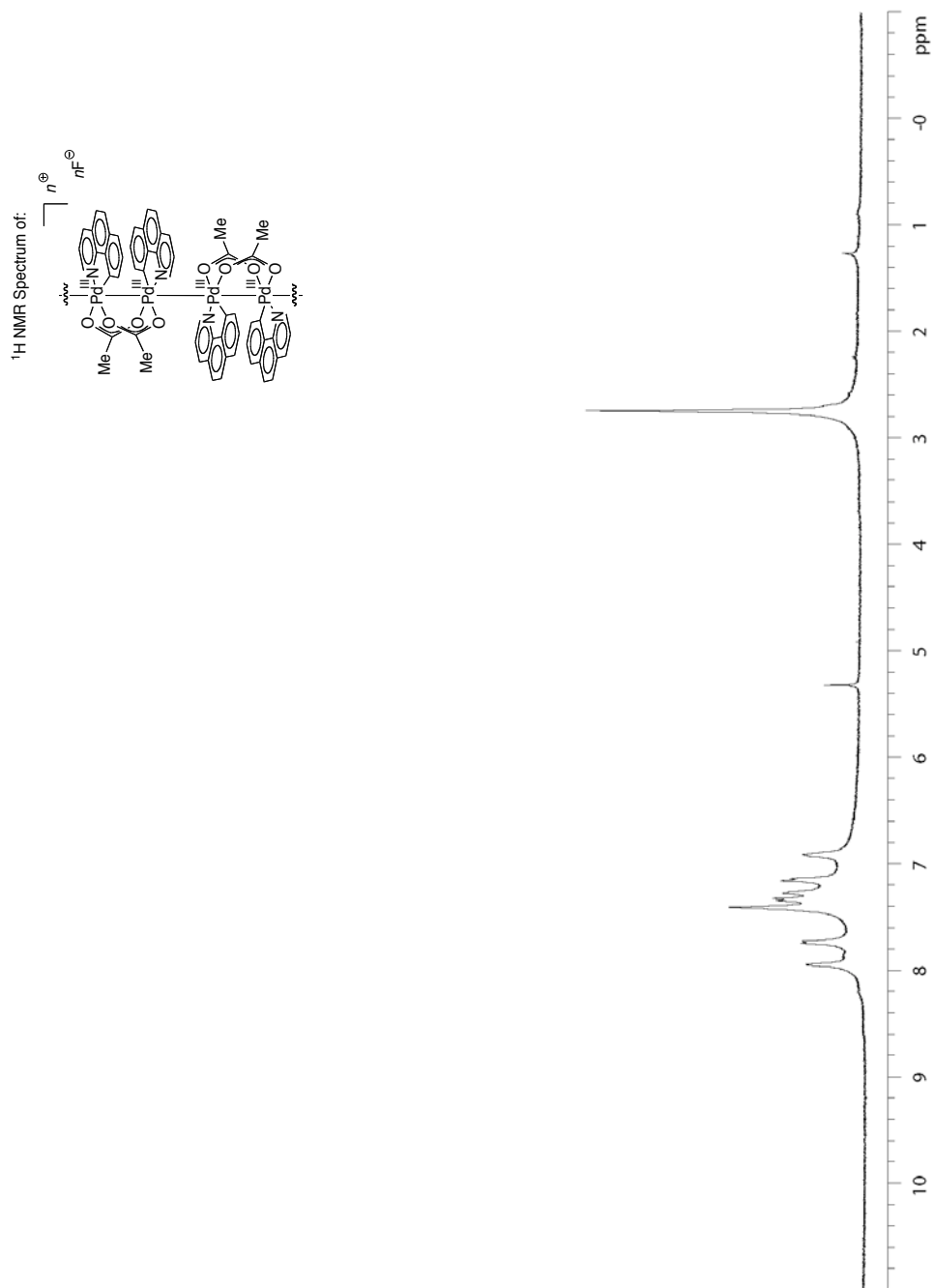
**NMR Data**

<sup>1</sup>H NMR of **1**. CDCl<sub>3</sub>, 500 MHz, 23 °C

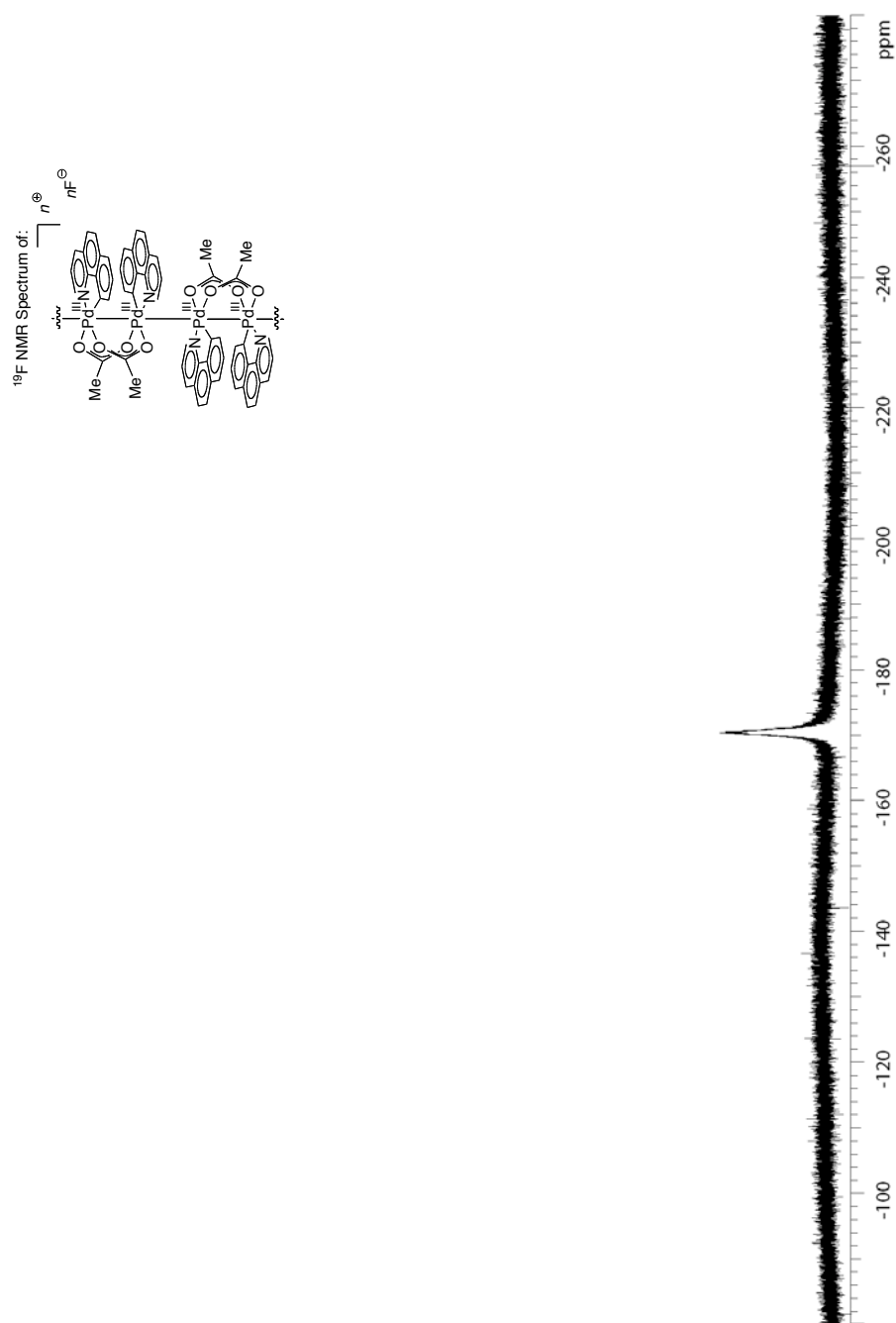


<sup>13</sup>C NMR of **1**. CDCl<sub>3</sub>, 125 MHz, 23 °C

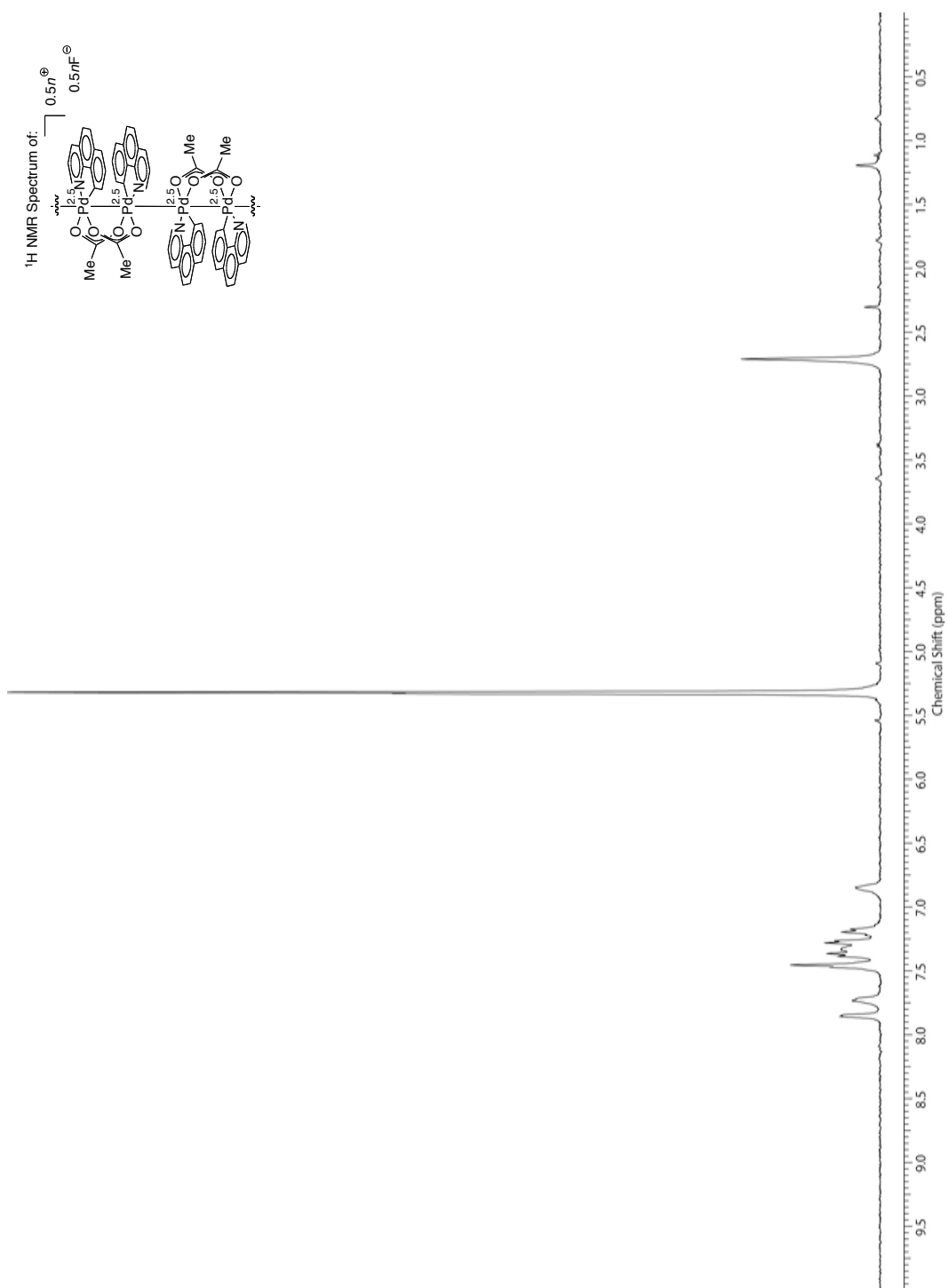




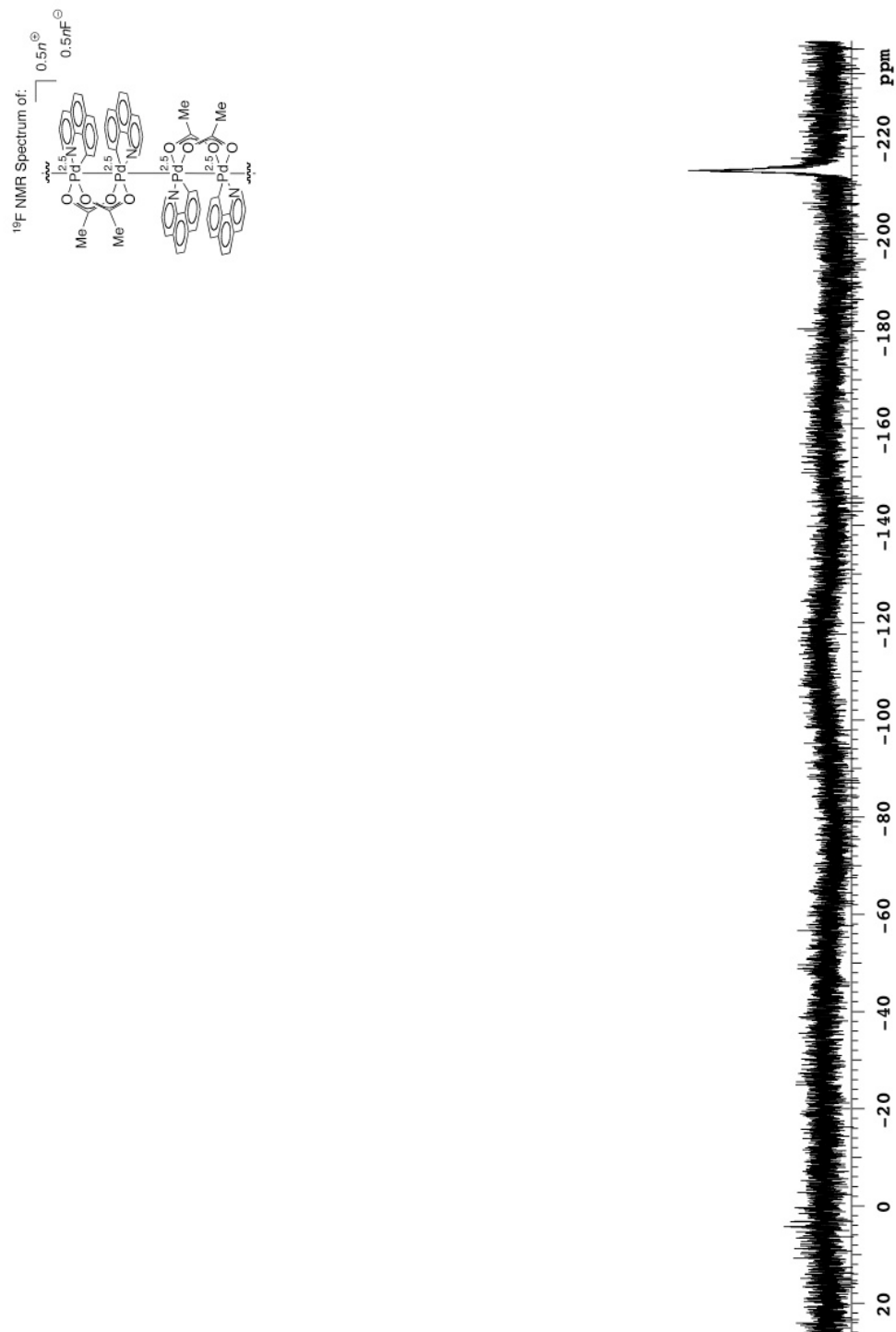
<sup>1</sup>H NMR of **2**. CD<sub>2</sub>Cl<sub>2</sub>, 400 MHz, -10 °C



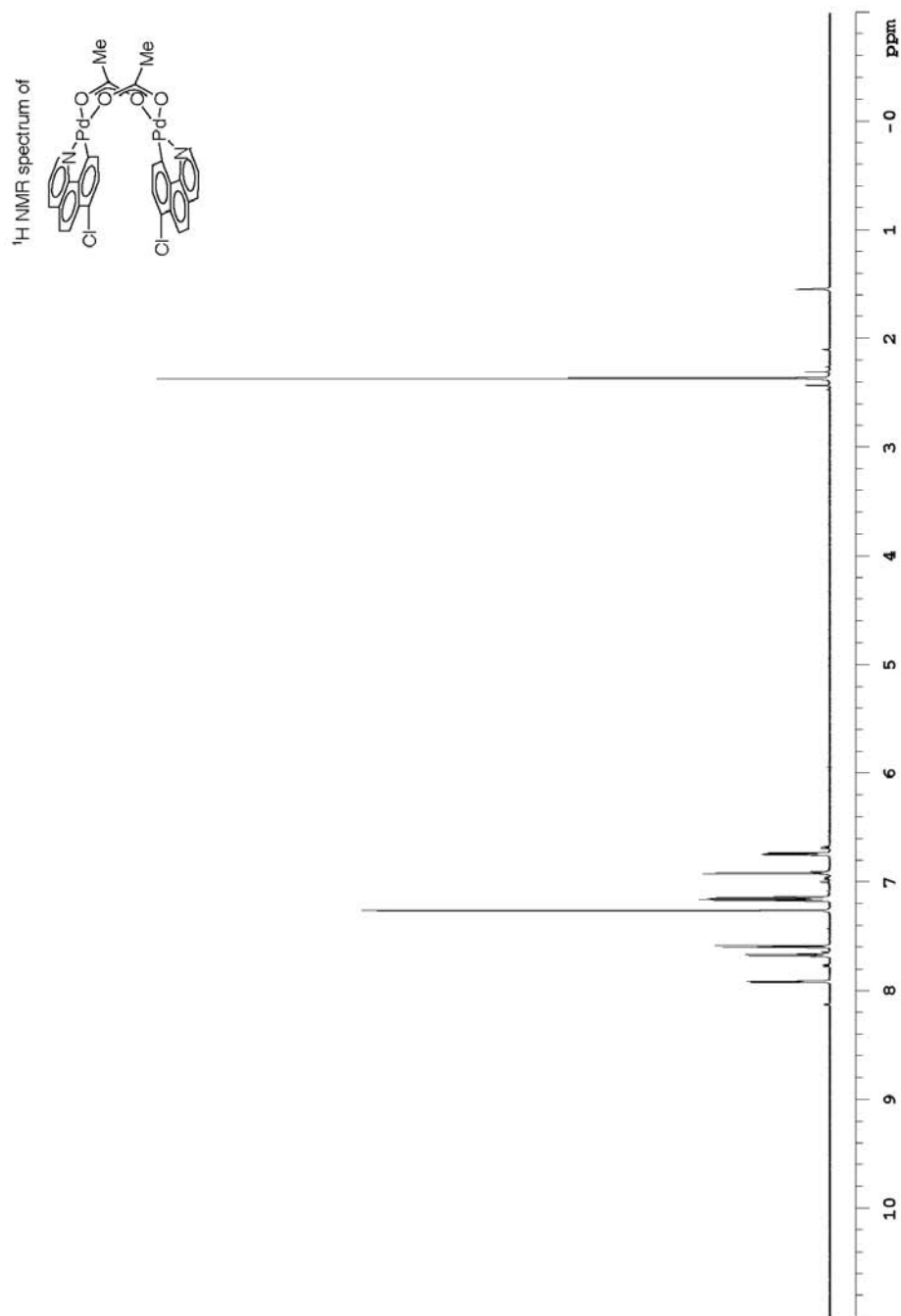
$^{19}\text{F}$  NMR of **2**.  $\text{CD}_2\text{Cl}_2$ , 375 MHz,  $-10\text{ }^{\circ}\text{C}$



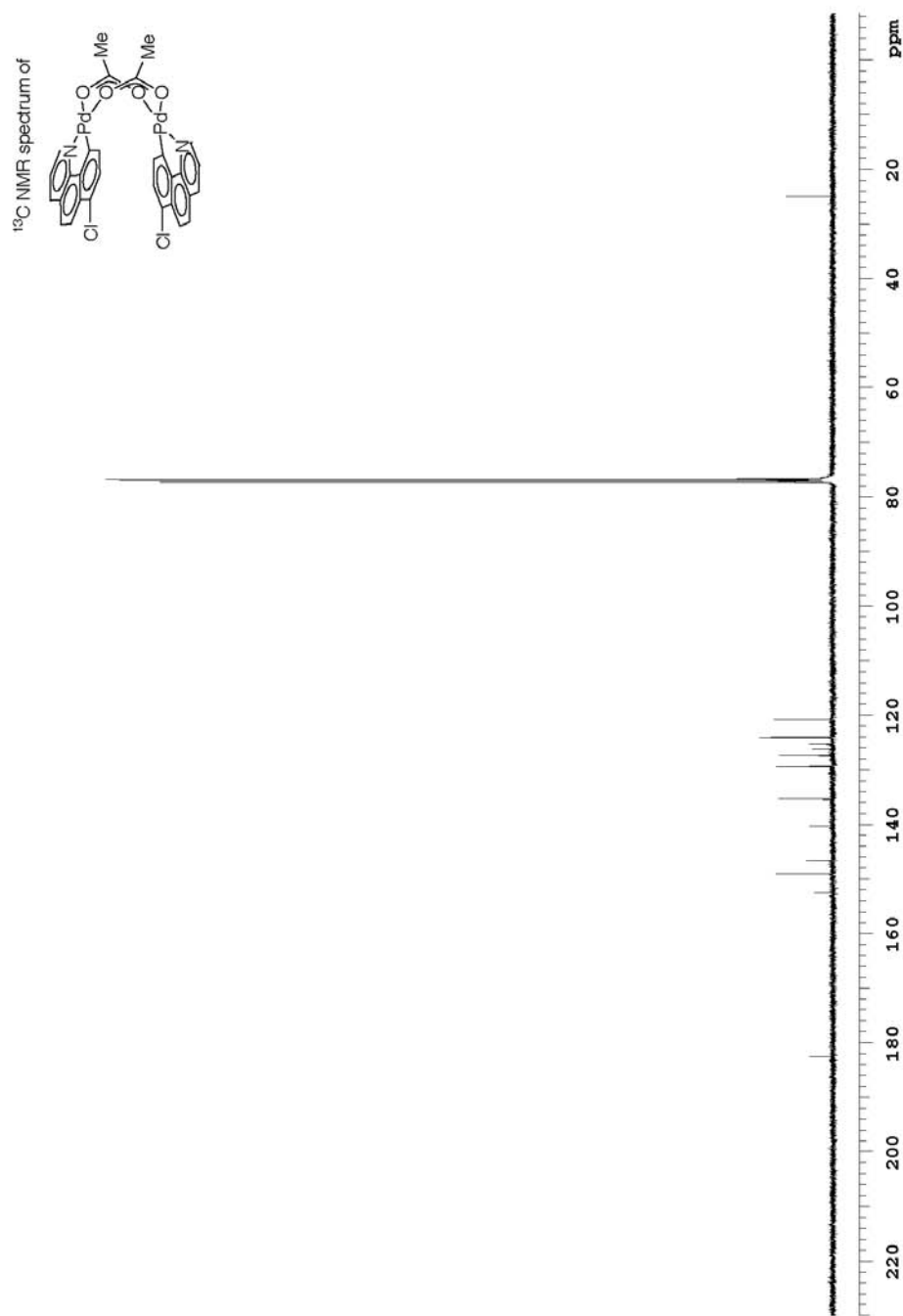
<sup>1</sup>H NMR of **3**. CD<sub>2</sub>Cl<sub>2</sub>, 400 MHz, -25 °C



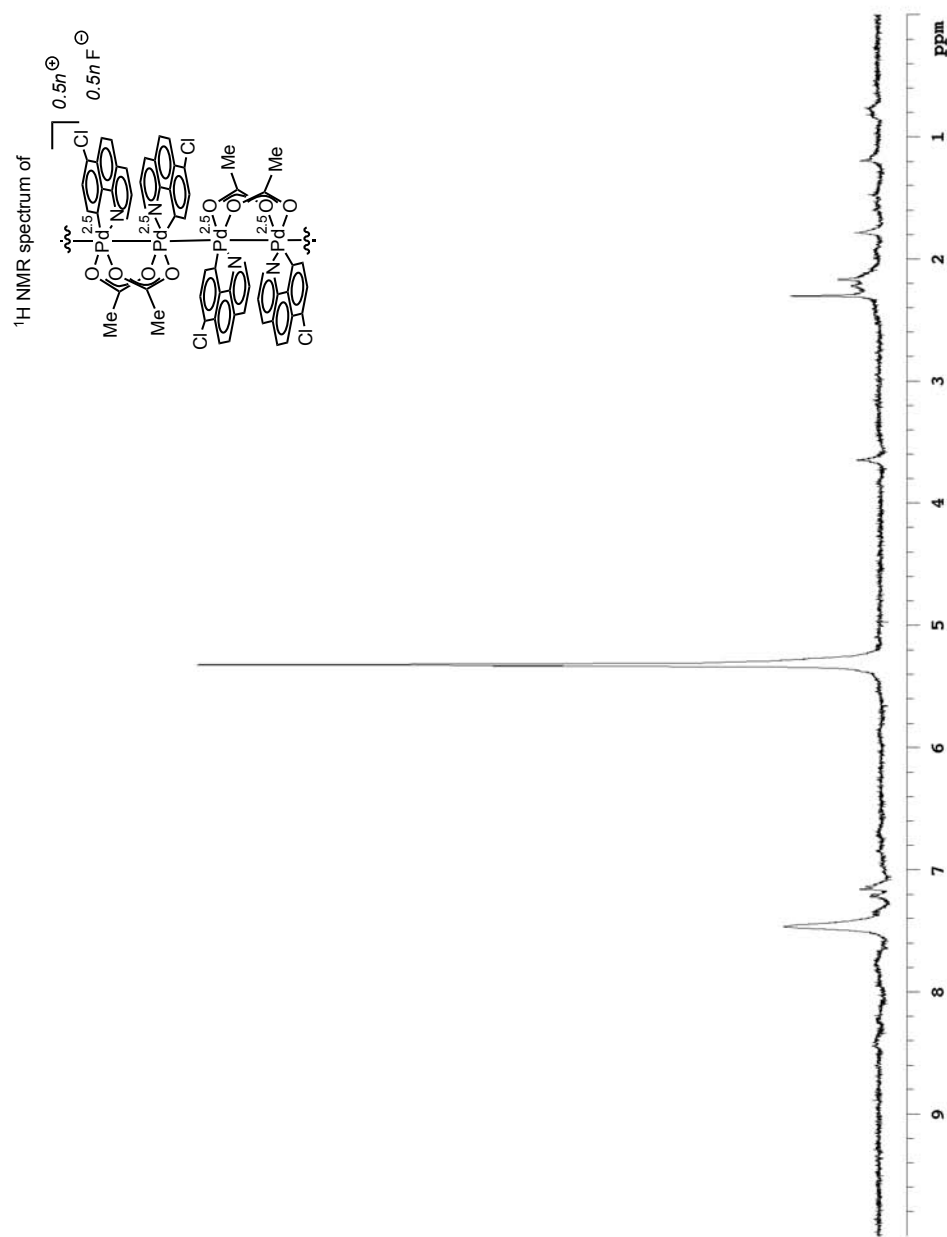
$^{19}\text{F}$  NMR of **3**.  $\text{CD}_2\text{Cl}_2$ , 375 MHz,  $-25\text{ }^\circ\text{C}$



<sup>1</sup>H NMR of **5**. CDCl<sub>3</sub>, 600 MHz, 23 °C

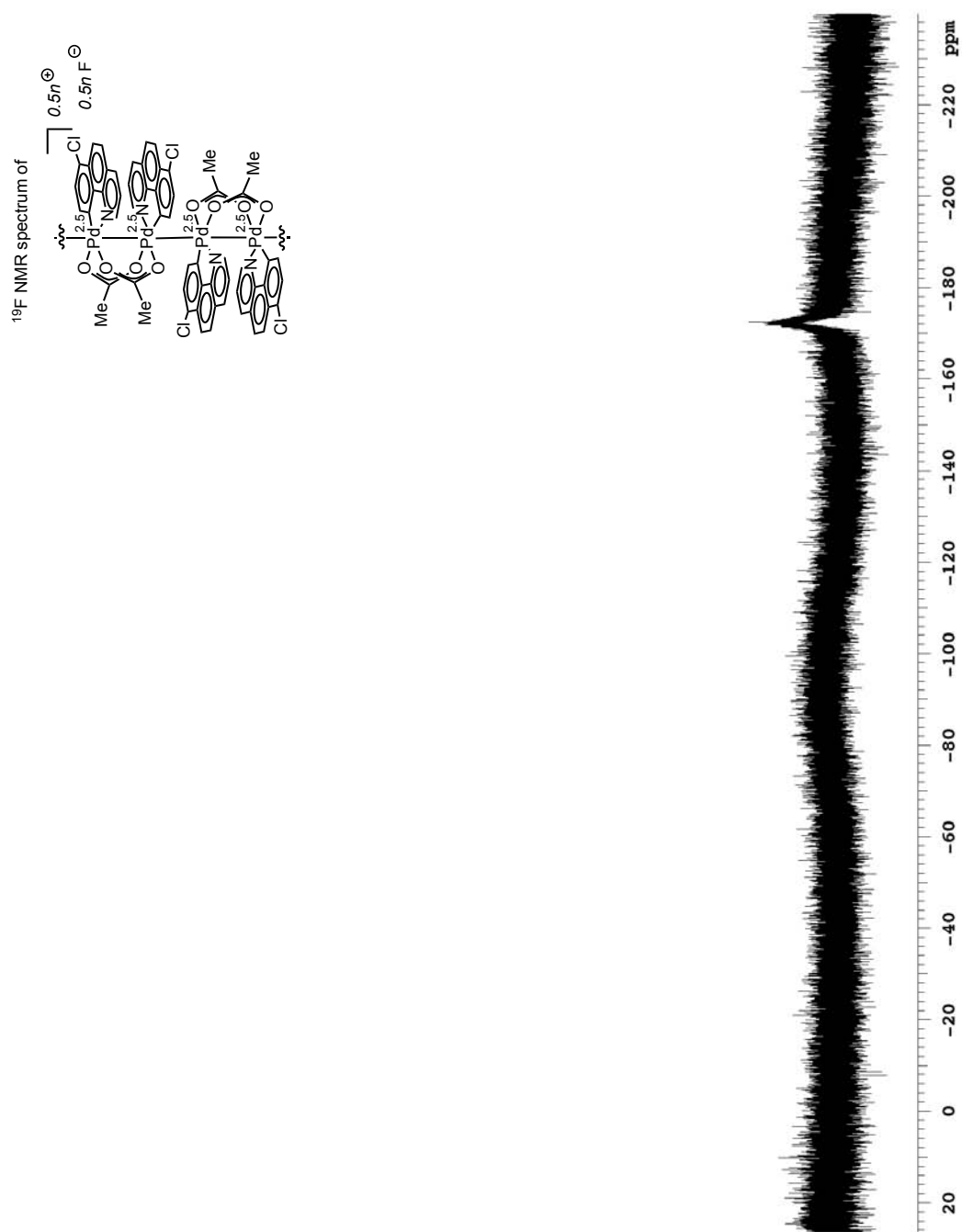


<sup>13</sup>C NMR of **5**. CDCl<sub>3</sub>, 125 MHz, 23 °C



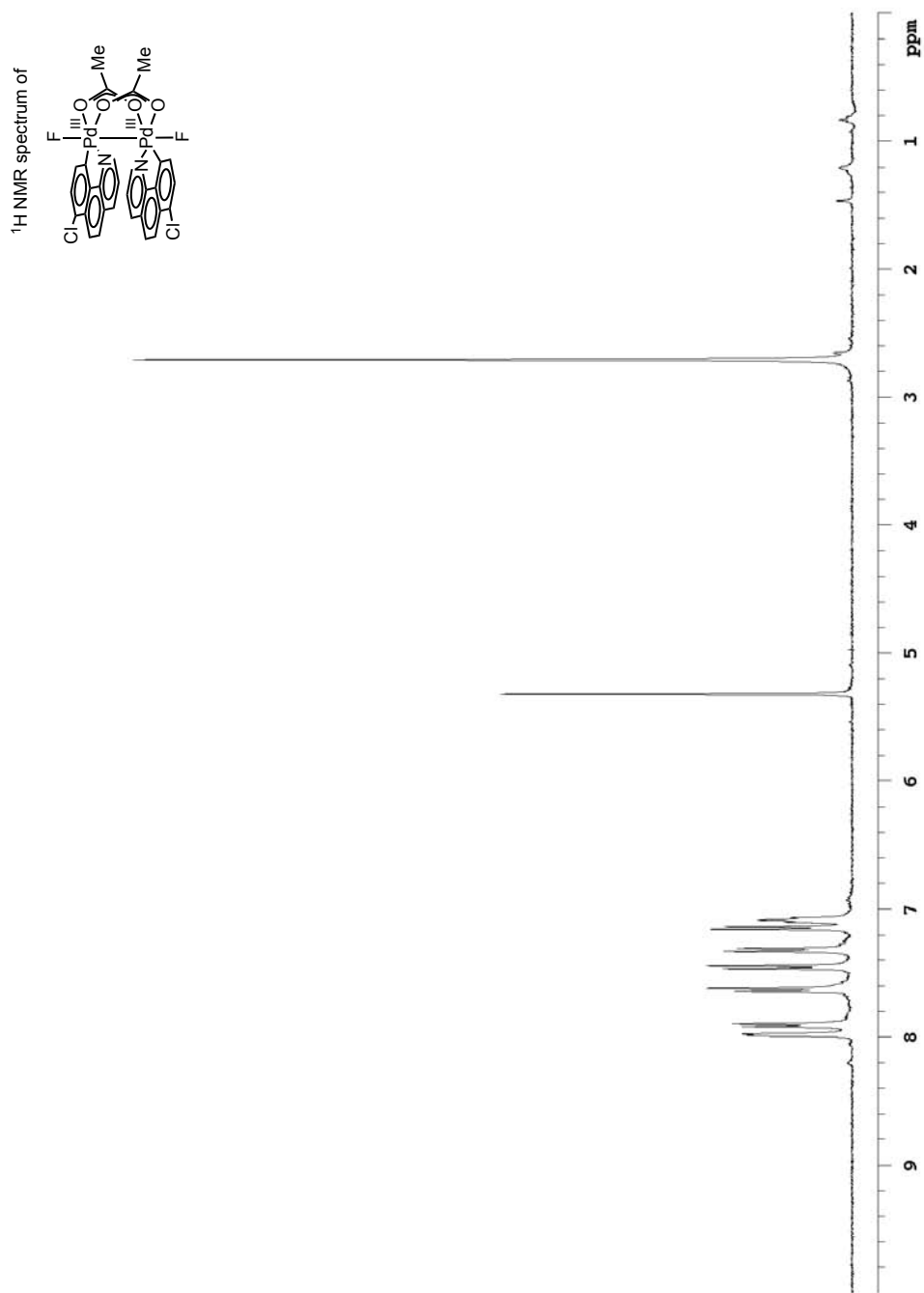
<sup>1</sup>H NMR of **6**. CD<sub>2</sub>Cl<sub>2</sub>, 400 MHz, -25 °C

The <sup>1</sup>H NMR spectrum for Pd(2.5) wire **6** displays very weak, broad signals that suggest a high degree of paramagnetism. This is in contrast to the <sup>1</sup>H NMR spectrum of Pd(2.5) wire **3**, which displays more well-behaved signals. Such a discrepancy suggests that alteration of the supporting ligand scaffold may also affect the degree of electronic communication between the dipalladium units of the 1-D Pd wires in solution.



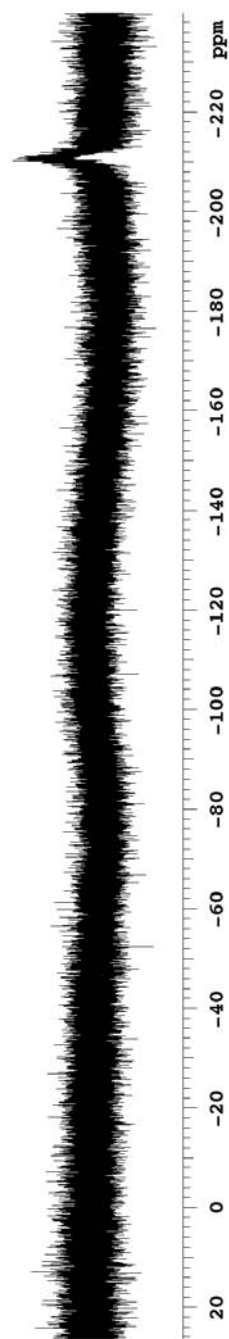
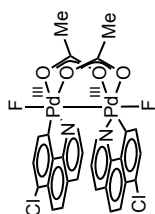
$^{19}\text{F}$  NMR of **6**.  $\text{CD}_2\text{Cl}_2$ , 375 MHz,  $-25^\circ\text{C}$





<sup>1</sup>H NMR of 7. CD<sub>2</sub>Cl<sub>2</sub>, 400 MHz, -25 °C

$^{19}\text{F}$  NMR spectrum of

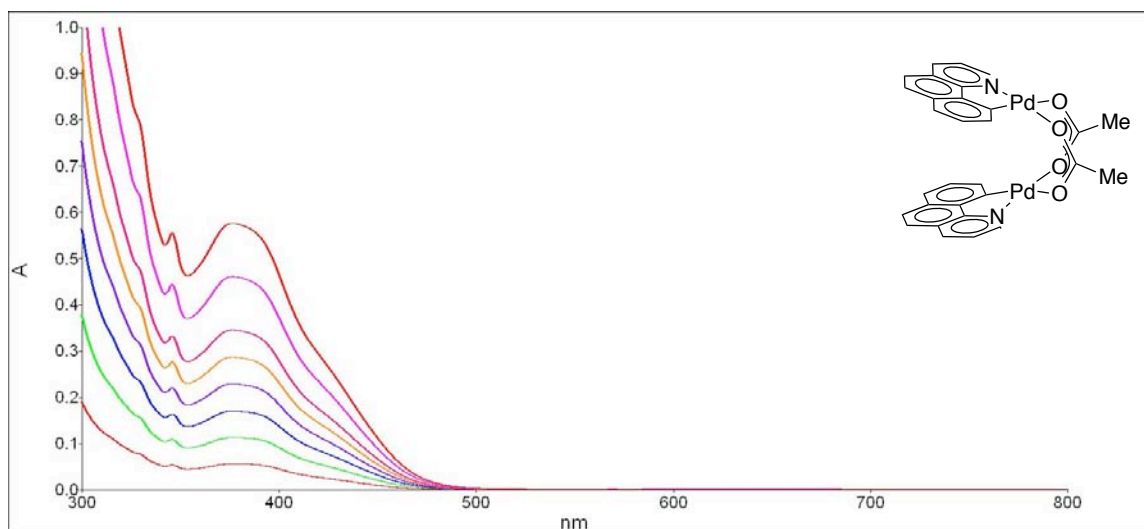


$^{19}\text{F}$  NMR of **7**.  $\text{CD}_2\text{Cl}_2$ , 375 MHz,  $-25\text{ }^\circ\text{C}$

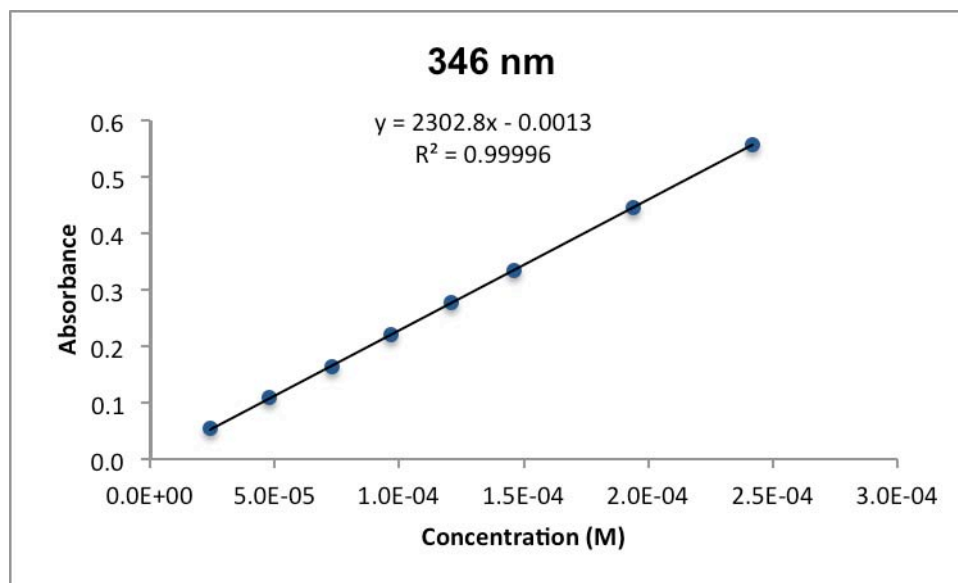
## UV-vis/NIR Data

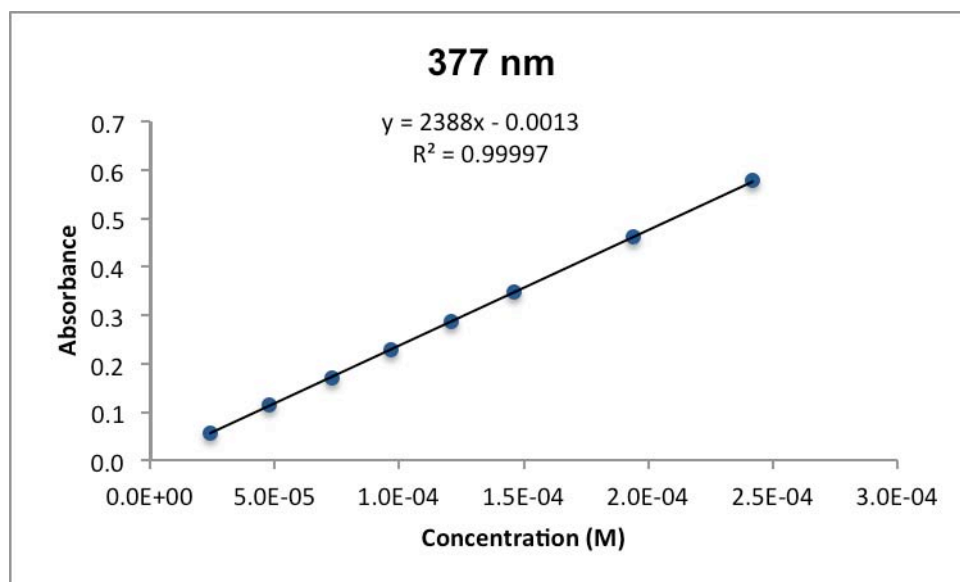
As a general note, all concentrations used in molar absorptivity determinations are molarity with respect to Pd. This is to facilitate comparison between species in which the aggregation state, and thus molecular weight, changes as a function of concentration (complexes **2**, **3**, **6** and **7**).

### UV-vis Spectrum of **1** (CH<sub>2</sub>Cl<sub>2</sub>, 23 °C)

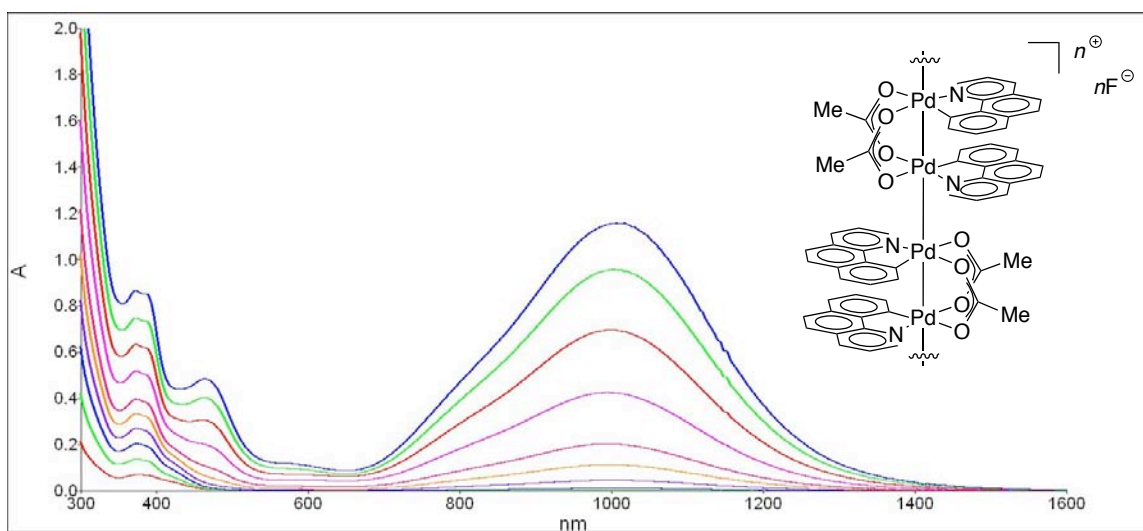


Molar Absorptivity Determinations:

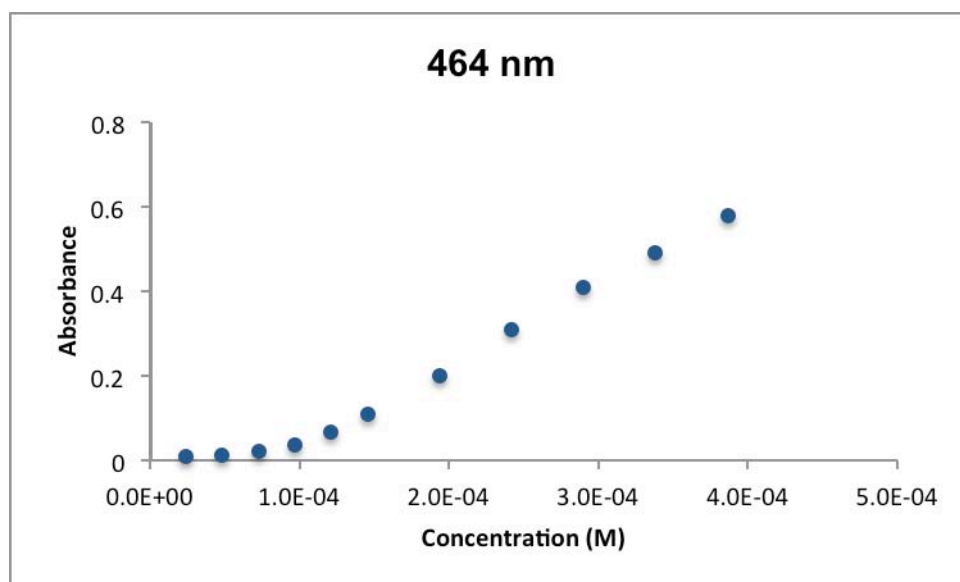
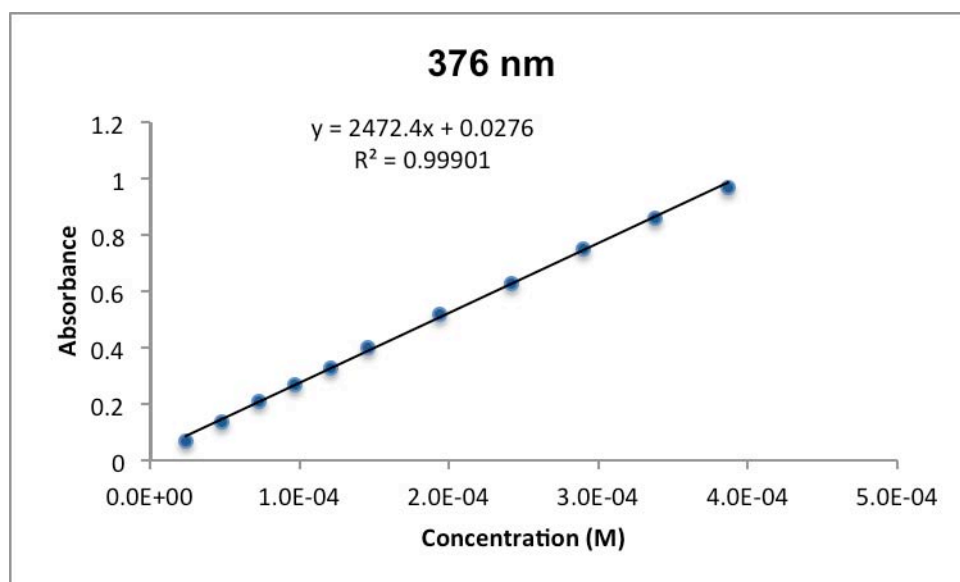


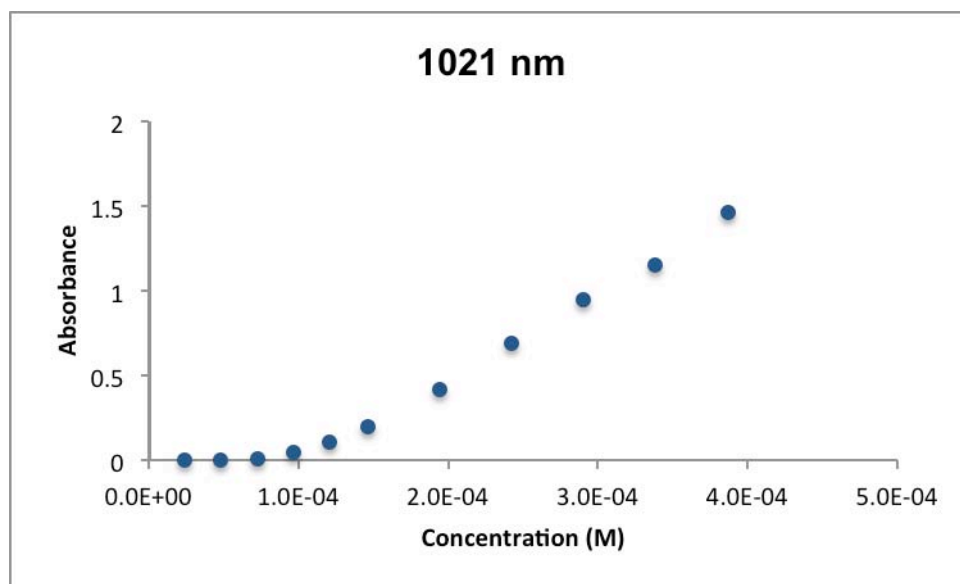


UV-vis/NIR Spectrum of **2** ( $\text{CH}_2\text{Cl}_2$ , 0 °C)



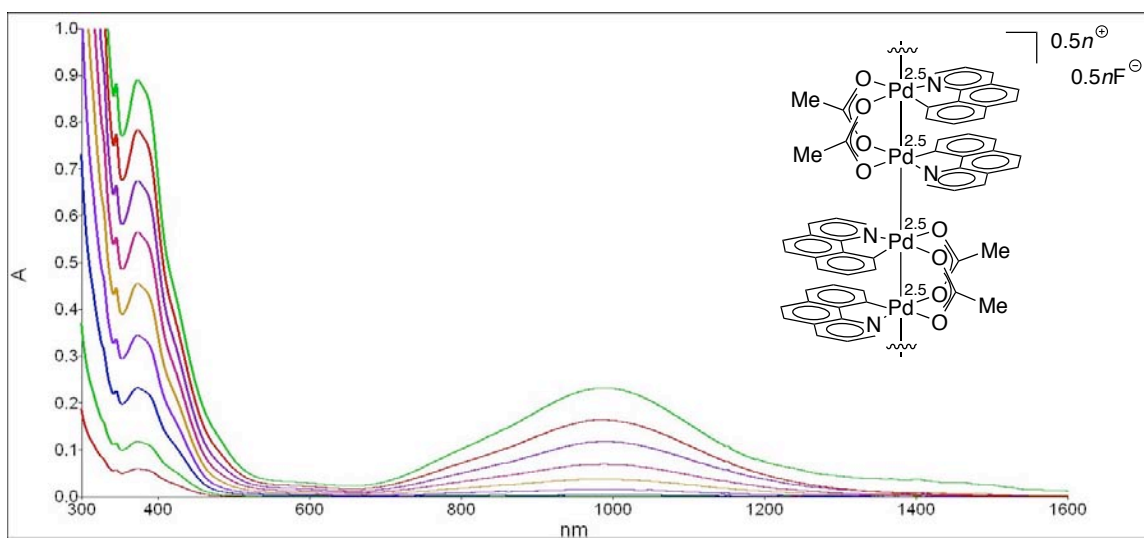
Molar Absorptivity Determinations:



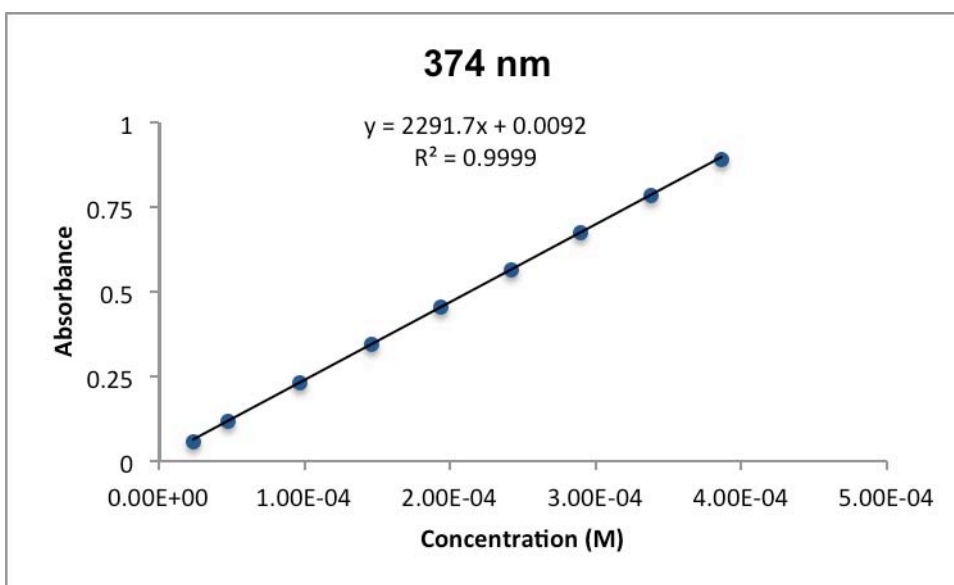
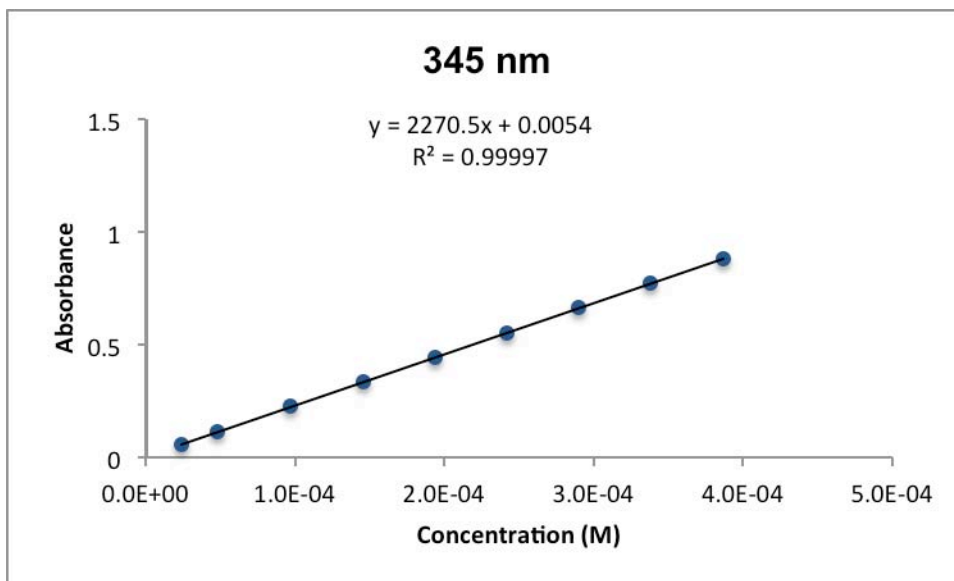


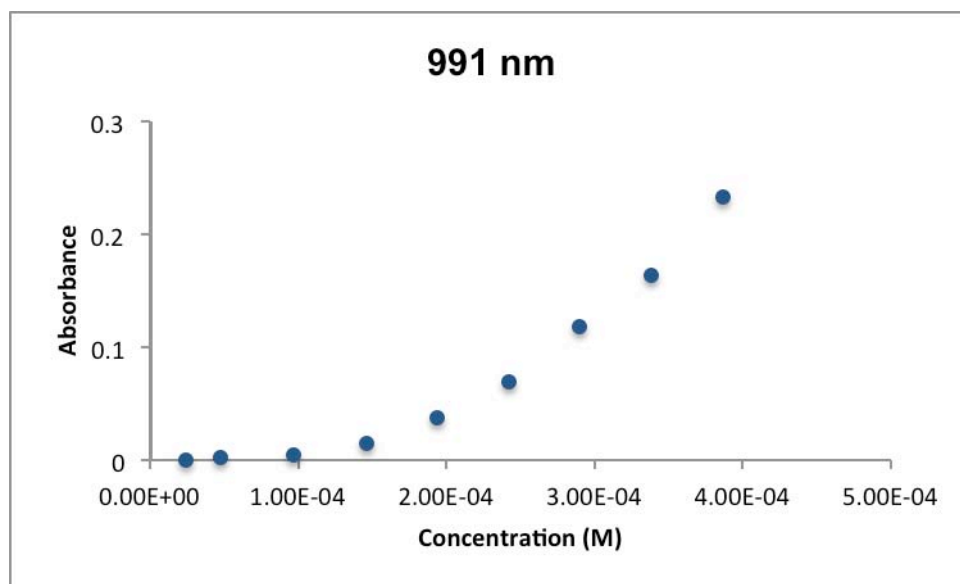
Absorbances at 464 and 1021 nm are non-linear with concentration. A curved absorbance vs. concentration plot is consistent with the formation of fluxional aggregates that increase in size with increasing solution concentration.

#### UV-vis/NIR Spectrum of **3** ( $\text{CH}_2\text{Cl}_2$ , $0^\circ\text{C}$ )



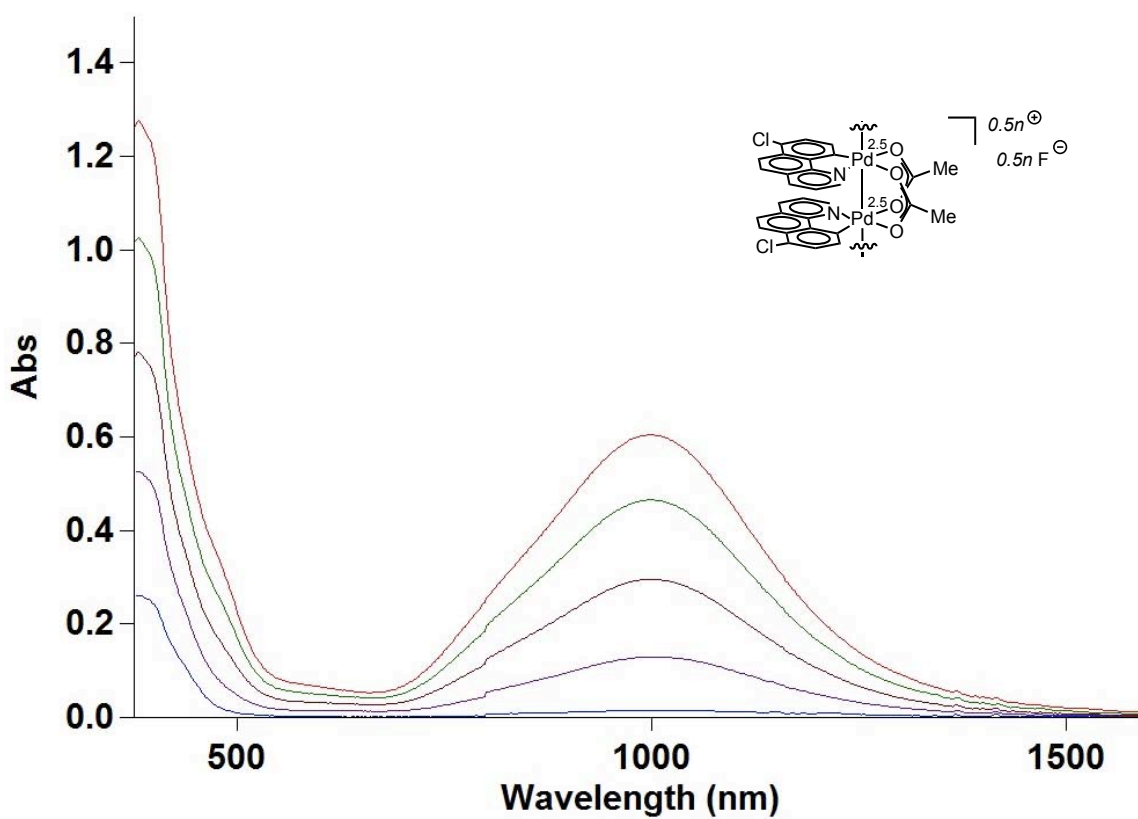
## Molar Absorptivity Determinations:





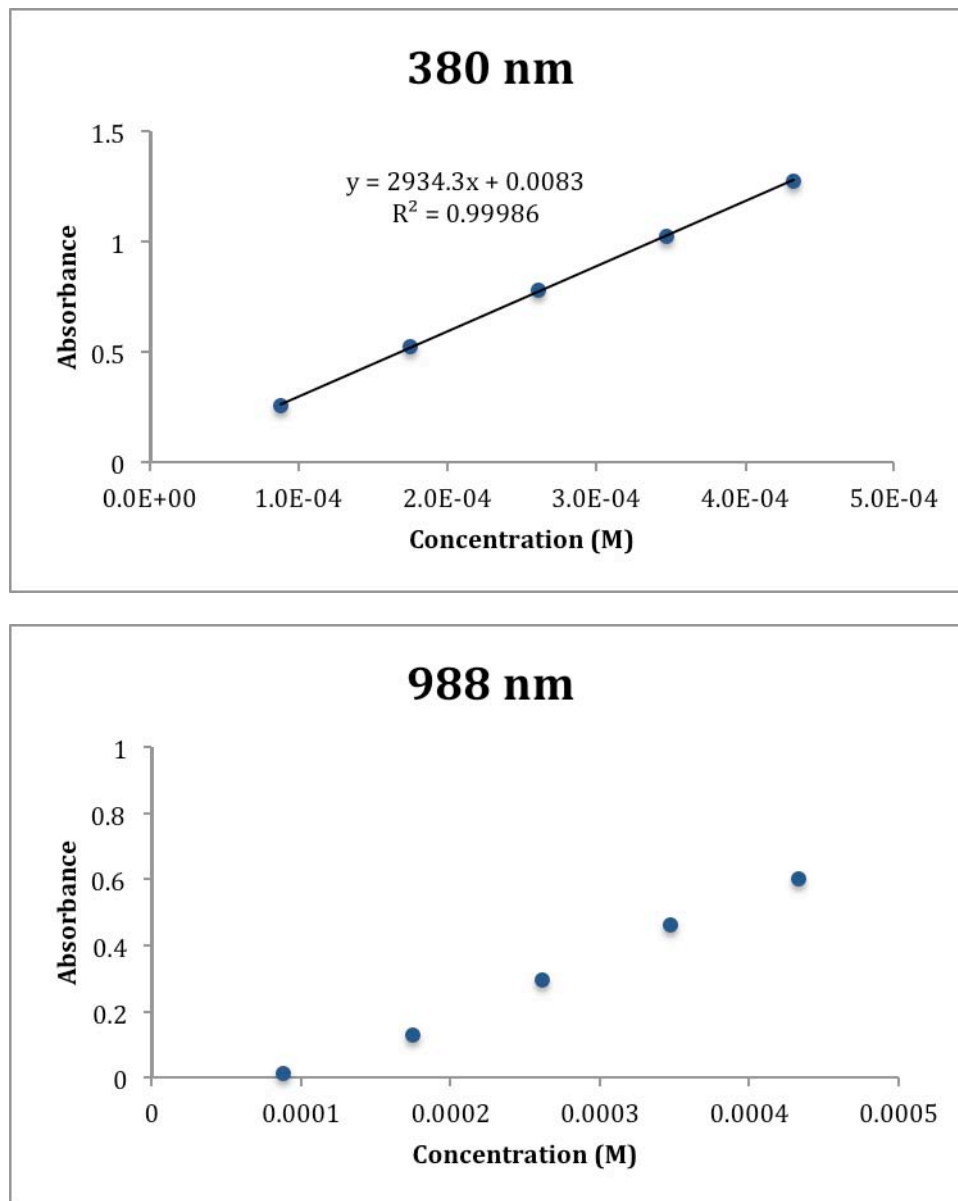
Absorbance at 991 nm is non-linear with concentration. A curved absorbance vs. concentration plot is consistent with the formation of fluxional aggregates that increase in size with increasing solution concentration.

#### UV-vis/NIR Spectrum of 6 ( $\text{CH}_2\text{Cl}_2$ , 5 °C)

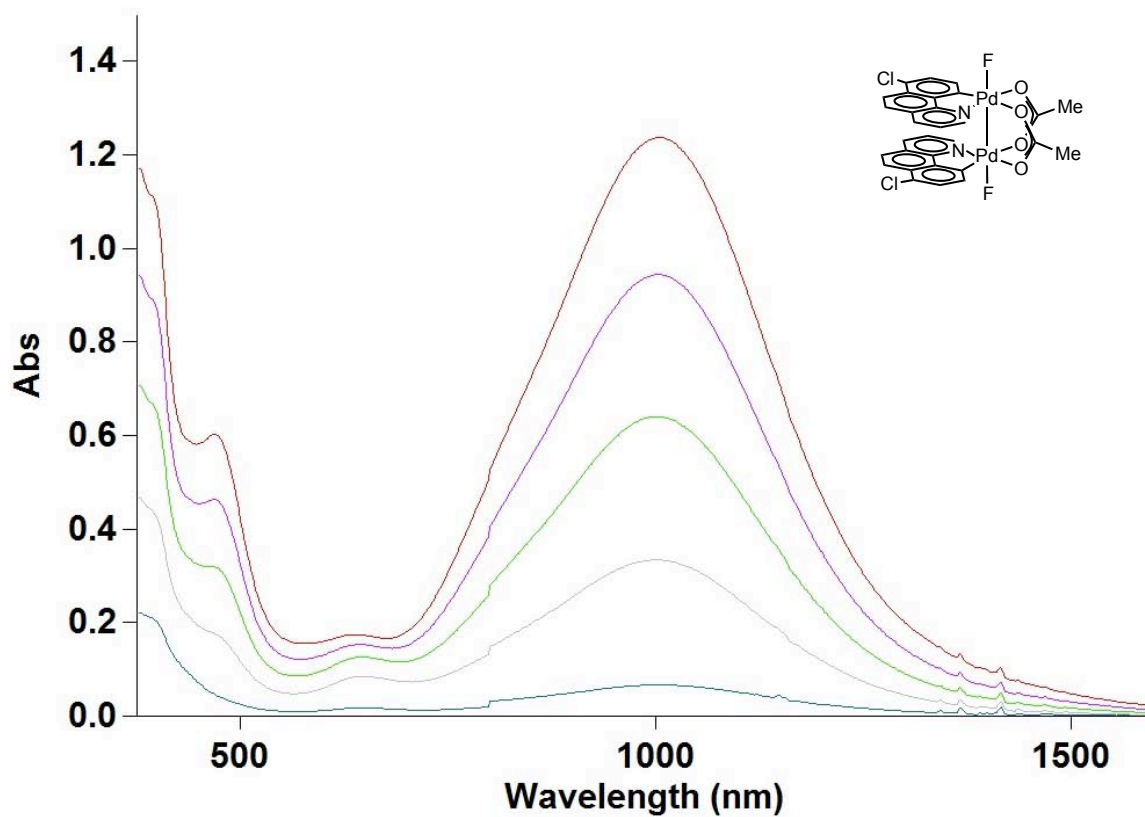




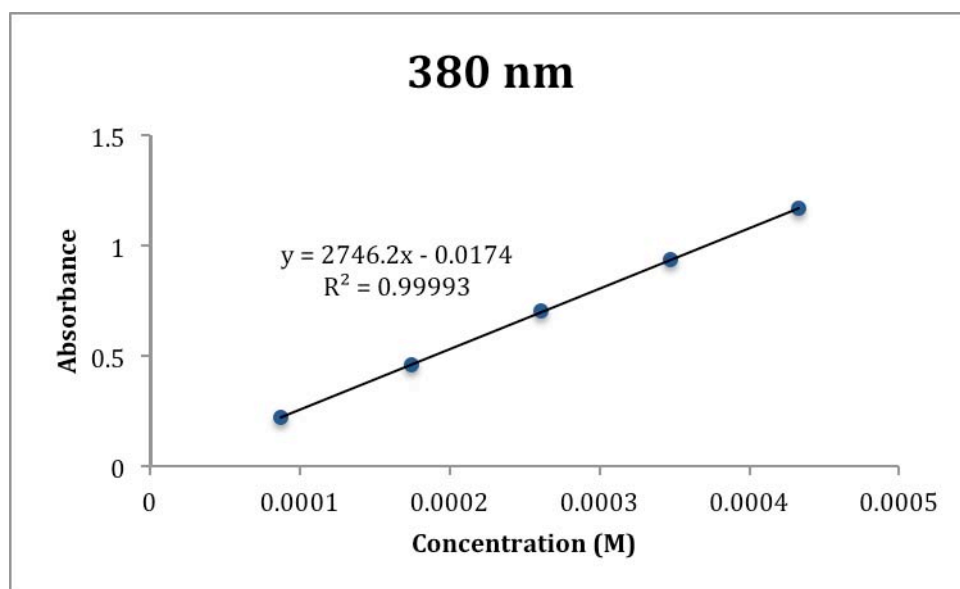
## Molar Absorptivity Determinations:

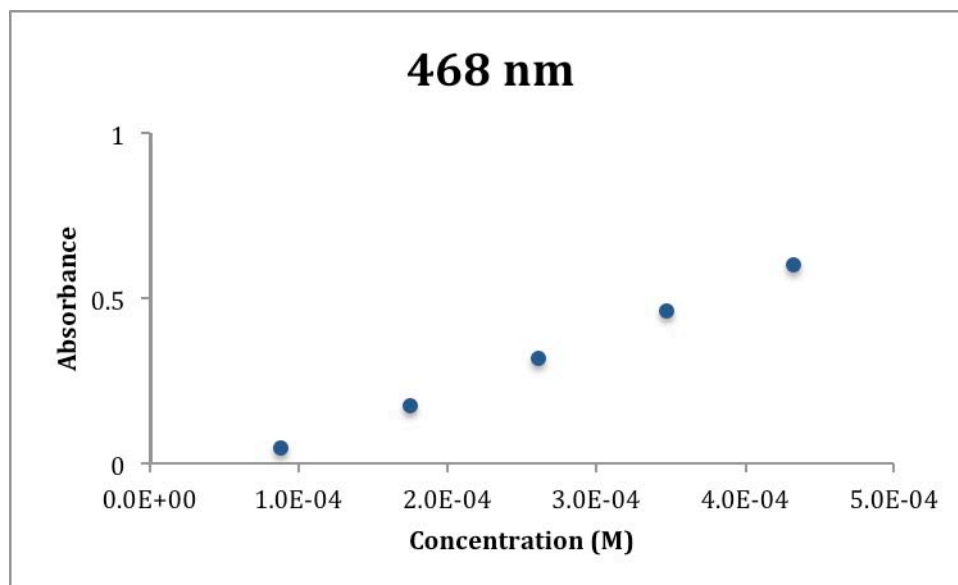
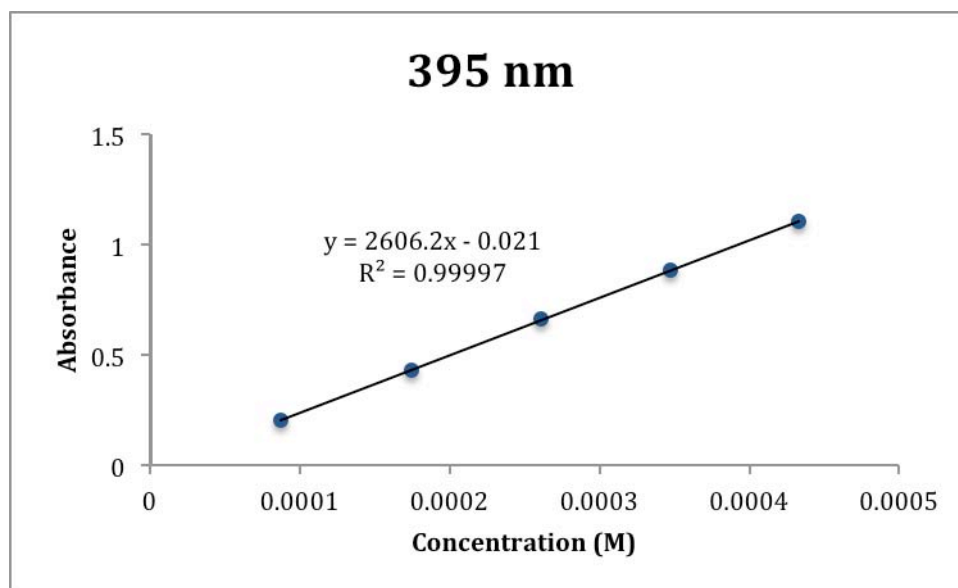


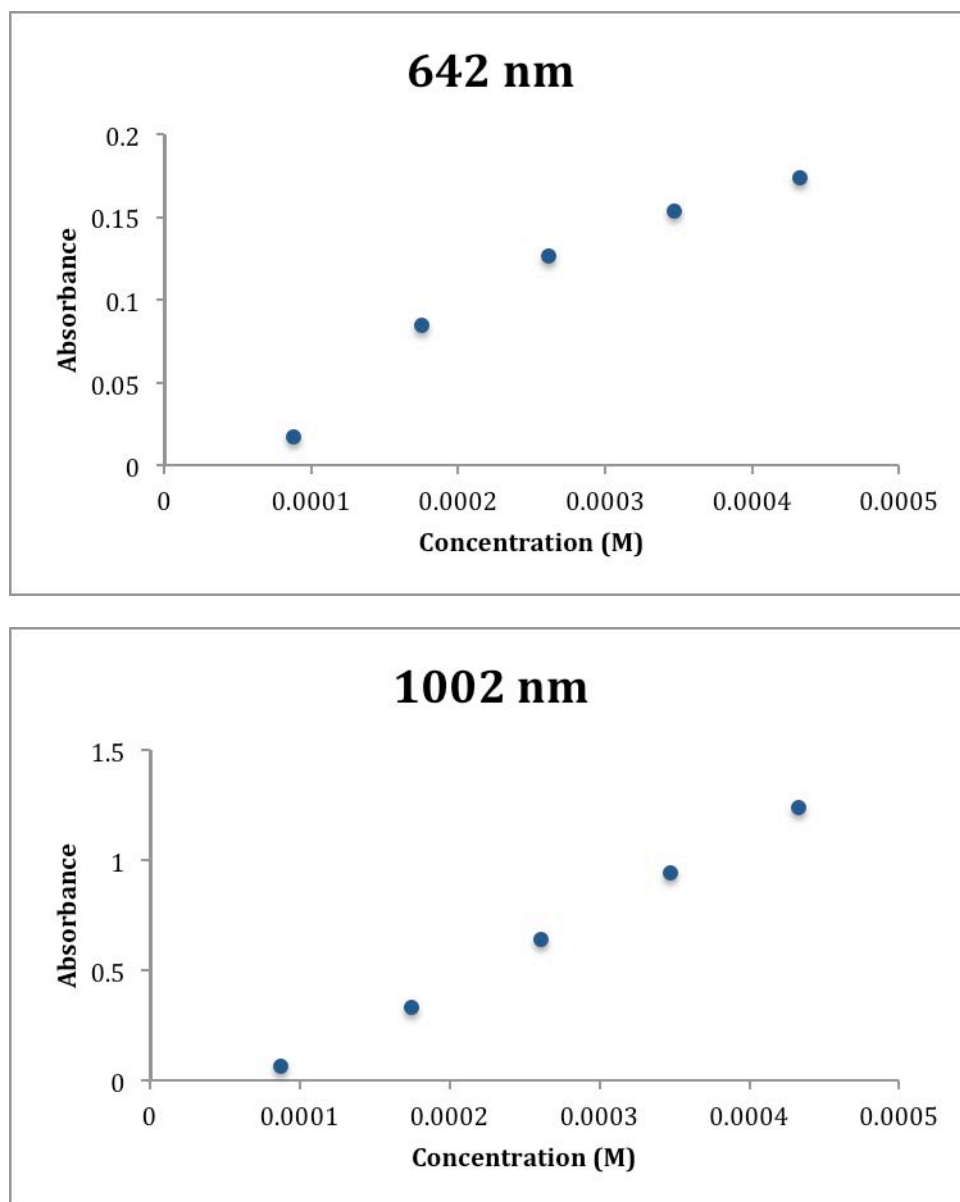
Absorbance at 988 nm is non-linear with concentration. A curved absorbance vs. concentration plot is consistent with the formation of fluxional aggregates that increase in size with increasing solution concentration.

UV-vis/NIR Spectrum of **7** (CH<sub>2</sub>Cl<sub>2</sub>, 5 °C)

Molar Absorptivity Determinations:







Absorbances at 1002, 642, and 468 nm are non-linear with concentration. A curved absorbance vs. concentration plot is consistent with the formation of fluxional aggregates that increase in size with increasing solution concentration.